Palaeogeography, Palaeoclimatology, Palaeoecology 417 (2015) 491–510

Contents lists available at ScienceDirect

Palaeogeography, Palaeoclimatology, Palaeoecology

journal homepage: www.elsevier.com/locate/palaeo

Palaeoenvironmental turnover across the Cenomanian-Turonian transition in Oued Bahloul, Tunisia: foraminifera and geochemical proxies

M. Reolid [a,*], C.A. Sánchez-Quiñónez [b], L. Alegret [c], E. Molina [c]

[a] Departamento de Geología, Universidad de Jaén, Campus Las Lagunillas sn, 23071 Jaén, Spain
[b] Departamento de Geociencias, Universidad Nacional de Colombia, Bogotá, Carrera 30, N° 45–03, Colombia
[c] Departamento de Ciencias de la Tierra e IUCA, Universidad de Zaragoza, Pedro Cerbuna 12, 50009 Zaragoza, Spain

ARTICLE INFO

Article history:
Received 9 April 2014
Received in revised form 6 October 2014
Accepted 10 October 2014
Available online 18 October 2014

Keywords:
Trophic conditions
Redox conditions
Ecostratigraphy
Foraminifera
OAE2
Cretaceous

ABSTRACT

The integrated analysis of foraminiferal assemblages, geochemical proxies, and stable isotopes in the Oued Bahloul section (Tunisia) allowed us to reconstruct the environmental turnover across the Cenomanian–Turonian boundary. An increase in palaeoproductivity proxies (P/Ti, U/Al, Sr/Al) and in $\delta^{13}C$ values, and a decrease in foraminiferal diversity and $\delta^{18}O$ values mark the beginning of the Oceanic Anoxic Event 2 (OAE2) at the *Rotalipora cushmani* and *Whiteinella archaeocretacea* biozones boundary. Eutrophic conditions at the seafloor and in the water column are evidenced by high proportions of buliminids and the replacement of planktic oligotrophic specialist *Rotalipora* by eutrophic opportunist *Hedbergella*. The enrichment in organic matter and redox sensitive elements, together with the abundance of low-oxygen tolerant benthic foraminifera, indicate dysoxic conditions in the deep-water column and at the seafloor (higher U_{aut} than Mo_{aut}). Among planktic foraminifera, deep- and intermediate-dwellers disappear (*Rotalipora* and *Globigerinelloides*), and surface-dwellers proliferate (*Hedbergella*). The persistency of the poorly oxygenated conditions during the *W. archaeocretacea* Biozone locally produced euxinic conditions where Mo_{EF} and Mo_{aut} reach high values, diversity presents minimum values, and benthic foraminifera temporarily disappear. The maximum percentage of heterohelicids indicates a stratified water column with a well-developed oxygen minimum zone. Improved oxygen conditions returned in the upper part of the *W. archaeocretacea* Biozone and *Helvetoglobotruncana helvetica* Biozone, with a slow recovery of foraminiferal assemblages, decrease in eutrophic genera (*Heterohelix*) and increase in mesotrophic genera (*Whiteinella*). A gradual increase in $\delta^{18}O$ values suggests decreased temperatures in surface waters. The OAE2 has been attributed to global temperature changes and palaeoceanographic reorganization. The poor mixing of surface and deep waters and enhanced primary productivity related to global warming – associated with increasing continental weathering and nutrient runoff – may have favored the eutrophication of the ocean and the expansion of the oxygen minimum zone.

1. Introduction

The Oceanic Anoxic Event 2 (OAE2), also called Bonarelli Event (e.g., Schlanger and Jenkyns, 1976; Arthur et al., 1990), is represented by the worldwide deposition of organic-rich facies close to the Cenomanian–Turonian (C-T) boundary. Two main hypotheses have been invoked to explain the deposition of organic-rich facies during the Cretaceous: (1) oceanic anoxia prevented the degradation of organic matter settling through the water column down to the seafloor by decreased oxygen supply to the deep ocean due to slower oceanic circulation (e.g. Erbacher et al., 2001; Tsandev and Slomp, 2009), or (2) enhanced surface water productivity exceeded the oxygen availability for decaying organic matter at the seafloor (e.g. Sarmiento et al., 1988; Handoh and Lenton, 2003). The OAE2 has been related to palaeoceanographic and climatic changes including greenhouse warming (e.g. Huber et al., 2002; Norris et al., 2002; Bornemann et al., 2008; Tsandev and Slomp, 2009; Monteiro et al., 2012; Pogge von Strandmann et al., 2013), a sea-level transgression (Hallam, 1992), a perturbation of the carbon cycle (e.g. Kuypers et al., 2002; Erba, 2004; Pogge von Strandmann et al., 2013) and a probable massive magmatic episode (e.g. Kuroda et al., 2007; Turgeon and Creaser, 2008; Erba et al., 2013). The planktic foraminiferal turnover (Coccioni and Luciani, 2004; Caron et al., 2006) includes the disappearance of genus *Rotalipora* close to the OAE2 (e.g. Hart, 1996, 1999; Nederbragt and Fiorentino, 1999; Keller et al., 2001; Coccioni and Luciani, 2004). Planktic foraminifera are sensitive to temperature, chemical and trophic conditions of the sea water (Caron, 1983; Caron and Homewood, 1983; Petrizzo, 2002;

* Corresponding author.
E-mail address: mreolid@ujaen.es (M. Reolid).

http://dx.doi.org/10.1016/j.palaeo.2014.10.011
0031-0182/

Gebhardt et al., 2004, 2010), and the ecostratigraphic analysis of their assemblages may be used to reconstruct palaeoceanographic and palaeoecological changes across the OAE2. In addition, the ecostratigraphic analysis of benthic foraminiferal assemblages is a useful tool to interpret fluctuations in oxygen and nutrient availability (e.g. Bernhard, 1986; Nagy, 1992; Jorissen et al., 1995; Van der Zwaan et al., 1999; Klein and Mutterlose, 2001; Reolid et al., 2008, 2012a, b). Some authors have interpreted an extinction event affecting benthic foraminiferal assemblages at the C-T boundary (e.g. Kaiho, 1994, 1999; Peryt and Lamolda, 1996; Peryt, 2004), yet there is no unanimity (Holbourn and Kuhnt, 2002).

The analysis of redox-sensitive trace elements (such as Co, Cr, Cu, Mo, and Ni, among others) has proven to be a powerful tool for interpreting redox conditions in oceans during anoxic events. These elements are less soluble under reducing conditions, resulting in synsedimentary enrichments under oxygen-depleted conditions (Wignall and Myers, 1988; Calvert and Pedersen, 1993; Jones and Manning, 1994; Powell et al., 2003; Gallego-Torres et al., 2007; Reolid et al., 2012a, b). Geochemical proxies have also been successfully applied to interpret palaeoproductivity, the most extensively used being Ba/Al, Sr/Al, Ca/Al and P/Ti ratios (e.g., Turgeon and Brumsack, 2006; Gallego-Torres et al., 2007; Robertson and Filippelli, 2008; Sun et al., 2008; Reolid and Martínez-Ruiz, 2012; Reolid et al., 2012a, b). The total organic carbon (TOC) has also been employed as an indirect palaeoproductivity proxy (e.g., Gupta and Kawahata, 2006; Su et al., 2008), although enhanced TOC contents may result from low bottom-water ventilation and oxygen depletion.

The aim of this work is to integrate planktic and benthic foraminiferal assemblages and geochemical proxies to determine the palaeoenvironmental turnover across the OAE2 in the Oued Bahloul section, Tunisia. The OAE2 and the C-T transition are recorded in the Bahloul Formation, where numerous studies on microfacies, planktic foraminifera, organic matter and stable isotopes have been carried out (e.g. Caron et al., 1999, 2006; Accarie et al., 2000; Amédro et al., 2005; Zagrarni et al., 2008; Negra et al., 2011; Soua et al., 2011; for recent works). Here we present the first integrated analysis of foraminiferal assemblages and geochemical proxies across the C–T transition at Oued Bahloul.

2. Geological setting and the Oued Bahloul section

The Cretaceous palaeogeography of Tunisia consists of three main domains: the Saharan Platform in the South, the Central Tunisian Platform, and the Tunisian Basin in the North (Burollet and Busson, 1983). The Central Tunisian Platform was mainly occupied by outer shelf facies rich in planktic foraminifera during the C-T interval. The Bahloul Formation is a widespread wedge that ranges from 23 m thick in the North to 2 m thick in the South, upon the Cenomanian Central Tunisian Platform (Saïdi et al., 1997; Scott, 2003; Robaszynski et al., 2010; Zaghbib-Turki and Soua, 2013; Fig. 1).

The Oued Bahloul section was proposed by Burollet (1956) as the type locality of the Bahloul Formation. This outcrop presents the best sedimentary record of the OAE2 in the southern margin of the Tethys (Robaszynski et al., 1993; Caron et al., 2006). The OAE2 is marked by a strong positive shift in $\delta^{13}C$ in bulk carbonate and an increase in organic matter content in the Bahloul Formation (Accarie et al., 1996; Nederbragt and Fiorentino, 1999). The studied interval is 47 m thick and includes the uppermost 5 m of the Fahdène Formation, the Bahloul Formation (29 m thick) and the lowermost 13 m of the Kef Formation (Fig. 1). The Fahdène Formation consists of an alternation of grey-greenish marls and light-coloured limestones. The Bahloul Formation is divided into two members: lower Pre-Bahloul Member and upper Bahloul *s. str.* Member (Fig. 1). In turn, the Pre-Bahloul Member is 3.4 m thick and its lower boundary with the Fahdène Formation is sharp and erosive. The first level (0.5 m thick) is a sandy micro-conglomeratic limestone that contains phosphatic black pebbles and quartz grains with well-developed graded bedding. The overlying bed is a bioclastic-rich calcarenite. The upper part of the Pre-Bahloul Member consists of marls with a decreasing content of quartz and bioclasts.

The Bahloul *s. str.* Member, in this work Bahloul Member, is composed of an alternation of 2 to 5 cm thick, bedded black limestones with thin parallel lamination, and grey marls. Different calcareous packages (50 cm thick) may be recognized where thin black limestones dominate versus intervals with dominance of grey marls. The lamination of the black limestones consists of clear laminae with abundant planktic foraminifera, and black laminae with abundant pellets embedded in a dark matrix with common radiolaria, benthic foraminifera (buliminids) and planktic foraminifera. The vertical transition from laminated black limestones to grey marls is gradual, but the transition from grey marls to black laminated limestones is abrupt. The top of the Bahloul Formation corresponds to densely bioturbated grey marls, and is locally overlain by a thin limestone layer rich in ammonoid moulds with phosphate and glauconite grains (Caron et al., 2006; Zagrarni et al., 2008). The overlying Annaba Member of the Kef Formation consists of grey marls with interlayered marly-limestones.

Robaszynski et al. (1990, 1993) located a sequence boundary at the top of Fahdène Formation, at the base of a channel-fill limestone bed (Ce SB5 *s.* Hardenbol et al., 1998). These authors situated the transgressive contact (Ce TS5) at the top of a thicker limestone bed, and the maximum flooding surface between the black laminated limestones of the Bahloul Formation and the marls of the Kef Formation.

3. Material and methods

Foraminiferal and geochemical analyses were conducted across the upper Cenomanian- lower Turonian at Oued Bahloul section. A total of 25 sampling levels were selected from this 47 m thick limestone and marly-limestone succession (Fig. 1). Micropalaeontological samples were disaggregated in water with diluted H_2O_2, washed through a 63 μm sieve, and dried at 50 °C. More endurated limestones were immersed in acetic acid (80%) during 1–4 h, depending on the carbonate content, then washed through a 63 μm sieve, and dried at 50 °C.

Quantitative studies (Tables 1 and 2) were based on representative splits (using a modified Otto microsplitter) of over 300 specimens of benthic foraminifera larger than 63 μm and 300 specimens of planktic foraminifera larger than 100 μm per sample. The remaining residue was scanned for rare species. Planktic foraminiferal taxa (Fig. 2) were also allocated to biserial (*Heterohelix*), triserial (*Guembelitria*), planispiral (*Globigerinelloides*), and trochospiral morphogroups (Table 3). The latter include strongly keeled (*Dicarinella*, *Rotalipora*, *Thalmanninella*), weakly keeled (*Anaticinella*, *Helvetoglobotruncana*, *Praeglobotruncana*) and unkeeled (*Hedbergella*, *Schackoina*, *Whiteinella*) forms (Table 3). Changes in depth stratification of the water column and trophic structure, temperature and salinity are the main factors controlling the composition of planktic foraminiferal assemblages. The stratification and richness of nutrients in the water column is narrowly related to productivity and the behavior of the planktic foraminifera. In this sense, opportunists (r-strategists) flourish in eutrophic waters whereas specialists (K-strategists) proliferate in oligotrophic waters (Valentine, 1973). Depth stratification favored differentiation of biotic and abiotic environmental features providing distinct ecological niches and minimizing the competition among species (Hemleben et al., 1989). Based on morphotype analyses (e.g. Corliss, 1985; Jones and Charnock, 1985; Corliss and Chen, 1988), benthic foraminiferal taxa (Fig. 3) were allocated to infaunal, epifaunal, and epifaunal/infaunal morphogroups. In general, benthic foraminifera with trochospiral, planoconvex or biconvex tests are inferred to have had an epifaunal mode of life, living at the sediment surface or in its upper few centimetres, while infaunal foraminifera have cylindrical or flattened tapered, spherical, globular unilocular or elongated multilocular tests, and live in the deeper layers of the sediment (Corliss, 1991; Reolid

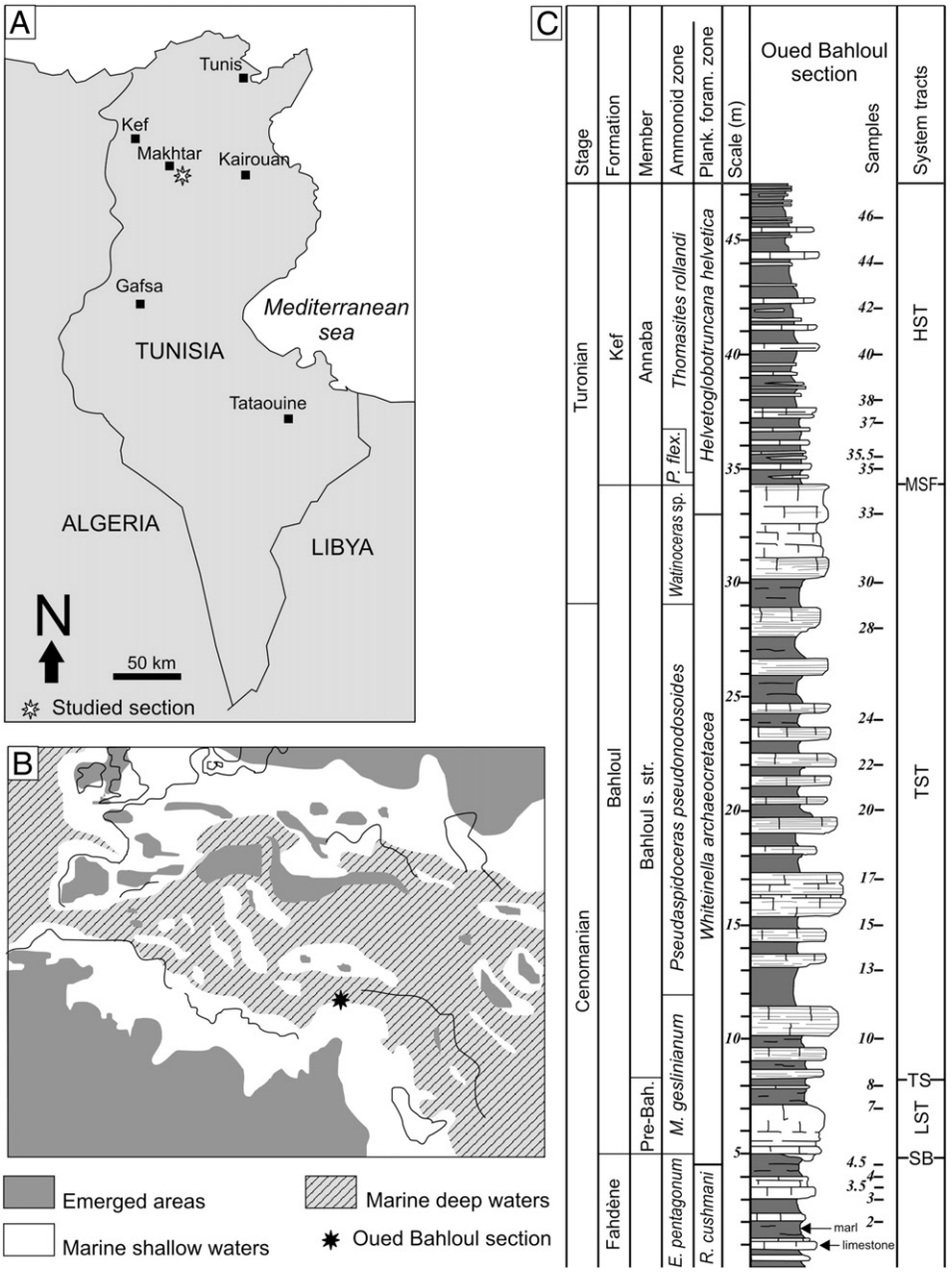

Fig. 1. (A) Geological setting, (B) palaeogeographic reconstruction of Western Tethys after Thierry (2000) and (C) Oued Bahloul section. Ammonite biostratigraphy according to Caron et al. (1999, 2006), Accarie et al. (2000), Amédro et al. (2005) and Zagrarni et al. (2008).

et al., 2008). Simple diversity (number of species) and the Fisher-α diversity index (e.g. Murray, 1991) were calculated separately for benthic and planktic foraminiferal assemblages.

Whole-rock analyses of major elements were carried out in 25 samples using X-ray fluorescence (XRF) in a Philips PW 1040/10 spectrometer. The content of trace elements was determined using an inductively coupled plasma-mass spectrometer (ICP-MS Perkin Elmer Sciex-Elan 5000) at the Centro de Instrumentación Científica (CIC, Universidad de Granada). Instrumental error was ±2% and ±5% for respective elemental concentrations of 50 ppm and 5 ppm.

The contents in C, N and S, as well as the total organic carbon (TOC) content, were analysed analyzed with an Elemental Analyzer LECO CNS-TruSpec and an Inorganic Carbon Analyzer CM5240 UIC in the laboratories of the Centro Andaluz de Medio Ambiente (CEAMA, Granada). Total organic carbon was obtained as the difference between total carbon and total inorganic carbon; it was measured in mg and calculated as percentage of sample weight.

For $\delta^{13}C$ and $\delta^{18}O$ analyses, and after roasting, the samples were reacted at 73 °C in an automated carbonate reaction system (Kiel-IV) coupled directly to the inlet of a Finnigan MAT 253 gas ratio mass spectrometer at the Laboratory of Stable Isotopes of the University of Michigan. Isotopic ratios were corrected for ^{17}O contribution and are reported in per mil notation relative to the VPDB standard. Values were calibrated using NBS 19 as the primary standard, and analytical precision was monitored by daily analyses of NBS powdered carbonate standards. The measured precision was maintained above 0.02‰ for $\delta^{13}C$ and $\delta^{18}O$.

In order to compare trace-element proportions in samples with varying carbonate and clay contents, trace-element concentrations were normalized to aluminium content (Calvert and Pedersen, 1993). This technique avoids any lithological effects on trace or major element concentrations, assuming that Al content in sediments is heightened by alumino-silicates (e.g., Calvert, 1990). The study of palaeoproductivity was carried out applying a set of proxies (Sr/Al, U/Al and P/Ti). To analyzse palaeo-oxygenation, diverse redox proxies evaluating the

Table 1
Planktic foraminiferal counts per sampling level.

Sample \ Species	*Anaticinella multiloculata*	*Dicarinella algeriana*	*Dicarinella hagni*	*Dicarinella imbricata*	*Globigerinelloides bentonensis*	*Globigerinelloides ultramicrus*	*Globoheterohelix paraglobulosa*	*Guembelitria cenomana*	*Hedbergella delrioensis*	*Hedbergella planispira*	*Hedbergella simplex*	*Helvetoglobotruncana helvetica*	*Helvetoglobotruncana praehelvetica*	*Heterohelix moremani*	*Heterohelix pulchra*	*Heterohelix reussi*	*Praeglobotruncana gibba*	*Praeglobotruncana stephani*	*Rotalipora cushmani*	*Rotalipora monsalvensis*	*Schackoina bicornis*	*Schackoina cenomana*	*Thalmanninella brotzeni*	*Thalmanninella greenhornensis*	*Whiteinella aprica*	*Whiteinella archaeocretacea*	*Whiteinella aumalensis*	*Whiteinella baltica*	*Whiteinella brittonensis*	*Whiteinella paradubia*	*Whiteinella* sp.	Total	N° Species	Fisher-alpha
OB10–46	0	4	0	0	0	0	26	0	82	19	4	1	26	6	8	166	9	17	0	0	0	1	0	0	14	0	0	38	9	0	0	430	16	4.28
OB10–44	0	3	0	0	0	0	66	6	19	8	1	0	13	4	0	189	0	5	0	0	0	0	0	0	5	7	0	26	3	0	0	355	14	2.92
OB10–42	0	5	0	0	0	0	37	17	57	5	3	3	11	0	1	111	1	14	0	0	0	0	0	0	50	19	0	66	4	0	0	404	16	3.32
OB10–40	0	0	0	0	0	0	3	0	0	0	0	1	2	0	0	7	7	30	0	0	0	0	0	0	192	17	0	37	54	3	0	353	11	2.16
OB10–38	0	3	1	0	0	0	10	21	41	38	3	8	11	4	0	56	22	28	0	0	0	0	0	0	111	17	0	20	17	0	0	411	17	3.57
OB10–37	0	0	0	0	0	0	15	0	31	7	5	25	22	0	0	43	17	16	0	0	0	0	0	0	142	0	0	35	28	0	0	386	12	2.36
OB10–35.5	0	0	0	0	0	0	20	68	73	17	17	3	2	4	1	62	5	13	0	0	2	0	0	0	63	2	0	18	13	0	0	383	17	3.64
OB10–35	0	5	3	1	0	0	19	25	61	15	0	7	20	3	0	104	7	20	0	0	0	0	0	0	19	8	0	25	0	0	0	342	16	3.52
OB10–33	0	1	2	0	0	0	27	70	21	19	0	3	15	2	0	96	0	2	0	0	0	0	0	0	37	4	0	20	2	0	0	321	15	3.26
OB10–30	0	0	0	0	0	0	32	8	25	17	0	0	10	5	0	113	3	0	0	0	0	0	0	0	22	62	0	43	10	0	0	350	12	2.4
OB10–28	0	0	0	0	2	0	0	7	22	23	0	0	7	1	0	122	0	6	0	0	0	1	0	0	49	73	0	16	12	0	0	341	13	2.68
OB10–24	0	0	0	0	0	0	0	4	4	20	0	0	23	8	0	82	2	1	0	0	0	0	0	0	37	79	0	12	26	0	0	298	12	2.51
OB10–22	0	0	0	0	0	0	0	7	14	27	0	0	2	38	0	219	0	0	0	0	0	0	0	0	22	34	0	27	9	0	0	399	10	1.85
OB10–20	0	0	0	0	0	0	0	12	7	35	0	0	18	13	0	133	0	0	0	0	0	0	0	0	41	89	0	17	6	0	0	371	10	1.89
OB10–17	0	0	0	0	0	0	0	0	4	10	0	0	0	1	0	54	0	0	0	0	0	0	0	0	1	0	0	0	0	0	0	70	5	1.23
OB10–15	0	0	0	0	0	0	1	2	4	30	0	0	0	18	3	209	0	0	0	0	0	0	0	0	0	0	0	0	0	0	0	267	7	1.32
OB10–13	0	0	0	0	0	0	0	0	4	40	4	0	0	35	0	265	0	0	0	0	0	0	0	0	0	0	0	0	0	0	0	348	5	0.83
OB10–10	0	0	0	0	0	0	11	0	17	21	0	0	3	10	1	68	0	0	0	0	0	0	0	0	3	3	4	3	2	0	0	146	12	3.21
OB10–8	0	0	0	0	3	2	0	14	89	22	12	0	1	4	3	98	0	0	0	0	0	0	0	0	6	12	2	26	24	0	0	318	15	3.27
OB10–7	0	0	0	0	1	1	0	0	22	1	0	0	0	0	0	1	0	0	0	0	0	0	1	0	6	0	0	0	0	0	0	33	7	2.77
OB10–4.5	0	0	0	0	14	1	0	0	57	27	5	0	0	0	0	9	0	12	1	0	0	0	59	1	5	4	0	6	0	0	3	204	14	3.43
OB10–4	0	0	0	0	47	3	0	0	143	12	17	0	0	3	3	56	2	22	6	12	0	0	21	11	0	0	4	0	4	0	0	366	16	3.43
OB10–3.5	1	1	0	0	78	8	0	0	90	25	25	0	0	3	0	25	10	35	2	15	0	0	19	15	0	2	3	4	2	0	0	363	19	4.29
OB10–3	0	0	0	0	80	16	0	0	42	123	34	0	0	5	0	79	0	17	12	8	0	0	11	8	0	0	0	0	0	0	0	435	12	2.29
OB10–2	0	0	1	0	32	31	0	5	89	80	38	0	0	6	1	52	3	12	6	5	0	0	9	4	0	0	0	6	0	0	0	380	17	3.61

relative increase of redox sensitive elements (Co/Al, Cr/Al, Cu/Al, Mo/Al, Ni/Al, and Th/Al) were applied throughout the section. Distinct enrichment factors (Mo and U), applied according to Zhou et al. (2012) and Trivobillard et al. (2012), included $Mo_{EF} = [Mo/Al]_{sample}/[Mo/Al]_{PAAS}$ and $U_{EF} = [U/Al]_{sample}/[U/Al]_{PAAS}$. The authigenic values of U and Mo were also calculated according to Zhou et al. (2012), as $Mo_{aut} = [Mo]_{sample}\text{-}[Mo]_{PAAS}/[Al]_{PAAS}{}^{*}[Al]_{simple}$, $U_{aut} = [U]_{sample}\text{-}[U]_{PAAS}/[Al]_{PAAS}{}^{*}[Al]_{simple}$.

4. Results

4.1. Planktic foraminifera and biostratigraphy

Planktic foraminifera dominate the assemblages in the Fahdène Formation (Fig. 4), where the P/B ratio is high (up to 93%). P/B values gradually decrease from the uppermost part of this formation towards the Bahloul Formation, with values commonly <30%, then gradually increase up to 98% towards the middle part of the Bahloul Formation (metre 17), remaining low (<30%) throughout the rest of the section and slightly increasing (up to 57%) in the lower part of the Kef Formation (Fig. 4).

A total of 13 genera and 31 species of planktic foraminifera were identified at Oued Bahloul (Fig. 2, Appendix 1). The species distribution allowed us to identify the *Rotalipora cushmani*, *Whiteinella archaeocretacea* and *Helvetoglobotruncana helvetica* biozones (Fig. 5). The upper Cenomanian *R. cushmani* Biozone corresponds to the lower part of the studied interval, and is mostly represented by the Fahdène Formation (Fig. 5). This interval contains abundant keeled trochospiral forms, such as *Rotalipora cushmani*, *Thalmanninella greenhornensis*, *Thalmannninella brotzeni*, *Rotalipora monsalvensis* and *Anaticinella multiloculata* (with a poorly developed keel). The *W. archaeocretacea* Biozone is 28 m thick, and it includes the uppermost 50 cm of the Fahdène Formation and the Bahloul Formation, containing the Cenomanian-Turonian boundary. This biozone is characterised by common biserial forms such as *Heterohelix reussi* and unkeeled trochospiral forms such as *Whiteinella archaeocretacea*, *Whiteinella aprica*, *Hedbergella planispira* and *Hedbergella delrioensis*. The *H. helvetica* Biozone (lower Turonian) is represented in the uppermost 1.2 m of the Bahloul Formation and in the Kef Formation. This biozone is characterised by the species *Helvetoglobotruncana helvetica*, *Dicarinella imbricata*, *Shackoina bicornis* and *Whiteinella paradubia*.

The correlation of the planktic foraminiferal and ammonite (Caron et al., 1999, 2006; Amédro et al., 2005) biozones is shown in Fig. 1C. The record of *Pseudocalycoceras angolaense* in the Pre-Bahloul Member and lowermost 3 m of the Bahloul Member indicates the *Metoicoceras geslinianum* Biozone (Cenomanian). The record of *Pseudaspidoceras pseudonodosoides* in the Bahloul Formation (12 to 29 m) indicates a late Cenomanian age (*P. pseudonodosoides* Biozone), and the record of *Watinoceras* and *Fagesia* in the topmost Bahloul Formation indicates early Turonian age (*Watinoceras* Biozone) (Fig. 1C). The base of the Kef Formation is lower Turonian in age: the *Pseudaspidoceras flexuosum* Biozone has been inferred by correlation with other sections (Accarie et al., 2000), and the *Thomasites rollandi* Biozone is indicated by the record of *Thomasites* sp. (Caron et al., 2006).

Diversity of planktic foraminiferal assemblages (Fig. 4) shows a decreasing trend from the Fahdène Formation towards the lower half of the Bahloul Formation (uppermost part of the *R. cushmani* Biozone and lower part of the *W. archaeocretacea* Biozone). Some taxa went extinct (e.g., *Globigerinelloides ultramicrus*, *Thalmanninella brotzeni*, *T. greenhornensis*, *Rotalipora cushmani*, *R. monsalvensis*), and others

Table 2

SAMPLE / SPECIES	*Ammodiscus* spp.	*Arenobulimina* spp.	*Astacolus* spp.	*Bathysiphon* spp.	*Bigenerina* sp.	*Bolivina* sp.	*Bolivinopsis* sp.	*Brunsvigella thoerensis*	*Charltonina australis*	*Chrysalogonium* sp.	*Conorotalites* sp.	*Cryptophragmium* spp.	*Dorothia pupa*	*Dorothia* spp.	*Frondicularia* sp.	*Gaudryina pyramidata*	*Gaudryina* spp.	*Gavelinella barremiana*	*Gavelinella cenomanica*	*Gavelinella flandrini*	*Gavelinella intermedia*	*Gavelinella rochardensis*	*Gavelinella* spp.	*Glandulina* sp.	*Globorotalites* sp.	*Globulina* spp.	*Gyroidinoides beissetl*	*Gyroidinoides globosus*	*Gyroidinoides lenticulus*	*Gyroidinoides* spp.	*Gyroidinoides subglobosus*	*Laevidentalina* spp.	*Lagena* spp.	*Lenticulina gaultina*	*Lenticulina* spp.
OB10-46	0	0	0	0	0	0	0	0	0	0	0	0	0	0	1	0	0	0	0	0	0	0	0	0	0	0	0	0	0	0	0	22	0	3	3
OB10-44	0	0	1	0	0	0	0	0	0	0	0	0	0	0	0	0	0	0	0	0	0	1	2	0	0	0	0	1	0	0	0	4	0	0	0
OB10-42	0	1	0	0	0	1	0	0	0	0	0	0	0	0	0	0	0	0	0	0	0	0	0	2	0	0	0	0	1	30	0	9	0	6	0
OB10-40	0	0	0	0	0	0	0	0	0	0	0	0	0	0	0	0	0	0	0	0	0	0	0	0	0	0	0	0	0	0	0	0	0	0	1
OB10-38	0	0	0	0	0	0	0	0	0	0	0	0	0	0	0	0	0	0	0	0	0	0	0	0	0	0	0	0	0	0	0	0	0	7	0
OB10-37	0	0	0	0	0	0	0	0	0	0	0	0	0	0	0	0	0	0	0	0	0	0	0	0	0	0	0	0	0	0	0	0	0	2	1
OB10-35.5	0	0	0	0	0	0	0	0	0	0	0	0	0	0	0	0	0	0	0	0	0	0	0	0	0	0	0	0	0	0	0	0	0	1	26
OB10-35	0	0	5	0	1	0	4	0	0	0	0	4	0	0	6	2	0	0	0	10	0	0	78	5	0	0	0	0	0	0	0	23	0	32	3
OB10-33	0	0	0	0	0	3	0	0	0	0	0	0	0	0	0	0	0	0	0	0	0	0	13	1	0	0	0	0	0	0	0	2	0	0	0
OB10-30	0	0	0	0	0	2	0	0	0	0	0	1	0	0	0	0	0	0	0	0	0	0	14	1	0	0	0	0	0	0	0	8	1	0	0
OB10-28	0	0	0	0	0	0	0	0	0	0	0	0	0	0	0	0	0	0	0	0	0	0	12	0	0	0	0	0	0	0	0	13	0	0	1
OB10-24	0	0	0	0	1	0	0	0	0	0	0	0	0	0	0	0	0	0	0	0	0	0	2	1	0	0	0	0	0	0	0	5	0	0	0
OB10-22	0	0	0	0	0	0	0	0	0	0	0	0	0	0	0	0	0	0	0	0	0	0	95	0	0	0	0	0	0	0	0	1	0	0	0
OB10-20	0	0	0	0	0	0	0	2	0	0	0	0	0	0	0	0	0	0	0	0	0	0	0	1	0	0	0	0	0	0	0	1	0	0	0
OB10-17	0	0	0	0	0	0	0	0	0	0	0	0	0	0	0	0	0	0	0	0	0	0	0	1	0	0	0	0	0	0	0	0	0	0	0
OB10-15	0	0	0	0	0	0	0	0	0	0	0	0	0	0	0	0	0	0	0	0	0	0	6	0	0	0	0	0	0	0	0	0	0	0	0
OB10-13	0	0	0	0	0	0	0	0	0	0	0	0	0	0	0	0	0	0	0	0	0	0	0	0	0	0	0	0	0	0	0	0	0	0	0
OB10-10	0	0	0	0	0	0	0	0	0	0	0	0	0	0	0	0	0	0	0	0	0	0	0	0	0	0	0	0	0	0	0	0	0	0	0
OB10-8	0	0	2	0	0	0	0	0	0	0	0	1	0	0	0	0	0	0	0	0	0	0	0	15	0	0	0	0	0	0	0	0	0	0	0
OB10-7	0	0	1	0	0	0	0	0	0	0	0	0	0	0	0	0	0	0	0	0	0	0	0	30	0	0	0	0	0	0	0	0	0	0	0
OB10-4.5	0	0	1	0	0	0	0	0	0	0	0	0	0	0	0	0	0	0	0	0	0	0	0	0	24	0	0	0	0	0	0	0	0	0	0
OB10-4	1	0	1	0	0	0	0	0	0	0	0	14	0	2	0	0	0	0	0	7	0	47	0	7	6	2	6	0	0	86	1	2	12	1	11
OB10-3.5	2	0	0	1	0	0	0	0	0	0	0	1	0	4	0	2	5	0	3	96	0	0	0	5	0	0	0	0	0	82	2	2	14	1	11
OB10-3	0	0	0	0	0	0	0	0	0	0	0	3	8	3	2	0	0	0	5	0	0	5	0	19	1	4	4	0	34	21	1	21	3	6	2
OB10-2	1	0	0	0	0	0	0	0	0	0	1	0	0	1	0	0	0	0	2	50	0	0	0	12	0	3	4	0	90	38	13	5	13	0	10	5

SAMPLE / SPECIES	*Lenticulina subgaultina*	*Lingulina* sp.	*Lingulina tricarinata*	*Lingulogavelinella frankei*	*Lingulogavelinella* sp.	*Marssonella oxycona*	*Neobulimina albertensis*	*Neobulimina irregularis*	*Neobulimina* spp.	*Neobulimina subregularis*	*Neoflabellina* sp.	*Palmula* sp.	*Plalmulina advena*	*Plalmulina dissona*	*Plalmulina* sp.	*Praebulimina* cf. *exigua*	*Praebulimina nannina*	*Praebulimina reussi*	*Praebulimina* spp.	*Pyrulina* spp.	*Pyrulinoides* spp.	*Quadrimorphina* sp.	*Quasispiroplectammina* spp.	*Rmmulina* spp.	*Reophax* sp.	*Remaniana charoides*	*Saracenaria* sp.	*Spiroplectammina* sp.	*Stensioeina excsulpta*	*Tappanina laticosa*	*Trappanina* sp.	*Textularia* sp.	*Trochammina globolaevigata*	*Vagninulina* sp.	*Valvulineria* sp.	*TOTAL*	No. Species	Fisher-alpha
OB10-46	0	0	0	0	0	3	178	3	1	7	0	0	0	0	0	35	0	11	0	0	0	0	0	0	0	0	0	0	0	39	0	1	0	0	0	*324*	14	2.98
OB10-44	0	0	0	0	0	0	4	5	0	2	0	0	0	10	0	33	0	8	0	1	0	2	0	0	0	0	0	0	0	4	0	0	0	0	0	*75*	12	4.11
OB10-42	29	1	0	0	0	1	74	0	0	2	0	0	1	0	4	0	0	29	0	0	1	0	0	0	0	0	0	0	1	32	0	0	0	0	0	*230*	19	4.94
OB10-40	0	0	0	0	0	0	2	0	0	0	0	0	0	15	1	0	0	0	0	0	0	0	0	0	0	0	0	0	0	0	0	0	0	0	0	*20*	5	2.24
OB10-38	0	0	0	0	0	0	4	0	0	1	0	0	3	4	0	0	0	0	0	0	0	0	0	0	0	0	0	0	0	1	0	0	0	0	0	*26*	8	4.08
OB10-37	1	0	0	0	0	0	12	0	0	0	0	0	0	0	0	0	0	0	0	0	0	1	0	0	0	0	0	0	0	0	0	0	0	0	0	*23*	8	4.69
OB10-35.5	26	0	1	0	0	0	10	0	0	3	0	0	14	0	8	0	0	26	0	0	0	0	0	0	0	0	0	0	0	76	0	0	0	0	0	*330*	11	2.19
OB10-35	0	0	0	0	0	0	10	0	0	3	0	0	0	0	4	0	0	0	0	0	0	0	0	0	0	0	0	0	0	25	0	0	0	0	0	*361*	21	4.87
OB10-33	0	0	0	0	0	0	133	2	0	6	0	0	2	0	4	0	0	50	0	1	0	0	0	0	0	0	0	0	0	30	0	0	0	0	0	*250*	14	3.21
OB10-30	0	0	0	0	0	0	10	0	0	0	0	0	0	0	0	0	0	0	0	0	0	0	0	0	0	0	0	0	0	20	0	0	0	0	0	*64*	11	3.83
OB10-28	0	0	0	0	0	0	7	0	0	0	0	0	3	0	0	15	0	0	0	0	0	0	0	0	0	0	0	0	0	6	0	0	0	0	0	*89*	9	2.49
OB10-24	0	0	0	0	0	0	275	2	0	31	1	0	0	0	0	12	0	0	1	0	0	0	0	0	0	0	0	0	0	0	0	0	0	0	0	*338*	12	2.44
OB10-22	0	0	0	0	0	0	177	37	1	14	0	0	0	0	0	1	0	0	0	0	0	0	0	0	0	0	0	0	0	0	0	0	0	0	0	*325*	6	1.04
OB10-20	0	0	0	0	0	0	88	2	0	34	0	0	0	0	0	0	0	1	0	0	0	0	0	0	0	0	0	0	0	25	0	0	0	0	0	*162*	9	2.12
OB10-17	0	0	0	0	0	0	0	0	0	0	0	0	0	0	0	0	0	0	0	0	0	0	0	0	0	0	0	0	0	0	0	0	0	0	0	*7*	1	0.93
OB10-15	0	0	0	0	0	0	93	6	0	4	0	0	0	0	0	0	0	4	0	0	0	0	0	0	0	0	0	0	0	30	0	0	0	0	0	*143*	6	1.29
OB10-13	0	0	0	0	0	0	83	0	0	5	0	0	0	0	0	0	0	4	0	0	0	0	0	0	0	0	0	0	0	0	0	0	0	0	0	*101*	3	0.57
OB10-10	0	0	0	0	0	0	249	15	0	31	0	0	0	0	0	0	0	0	0	0	0	0	0	0	0	0	0	0	0	0	0	0	0	0	0	*295*	3	0.46
OB10-8	0	0	0	0	0	0	38	0	0	0	0	0	0	0	0	0	0	33	12	0	0	0	0	0	0	0	0	0	0	2	0	9	0	0	0	*138*	11	2.84
OB10-7	2	0	0	0	0	0	0	0	0	0	0	0	0	0	0	0	0	0	0	0	0	0	0	0	0	0	0	0	0	0	0	0	0	0	0	*54*	9	3.04
OB10-4.5	0	0	0	0	0	0	0	0	0	0	0	0	0	0	0	0	0	3	0	0	0	0	0	0	0	0	0	0	0	0	0	0	0	0	0	*125*	16	4.93
OB10-4	1	0	0	0	0	0	0	0	0	0	0	0	0	0	0	0	0	30	0	3	15	0	0	0	0	0	0	0	0	0	0	0	35	0	1	*322*	25	6.31
OB10-3.5	0	0	0	0	0	0	0	0	0	0	0	0	0	0	0	0	0	3	11	0	3	2	0	0	0	0	0	0	0	0	0	4	13	0	0	*308*	30	8.25
OB10-3	0	0	0	0	0	0	0	0	0	0	0	0	0	0	0	0	0	4	29	2	2	14	0	8	0	0	0	0	0	0	0	1	30	0	0	*253*	30	8.97
OB10-2	0	0	0	0	0	0	0	0	0	0	0	0	0	0	0	0	0	1	7	0	0	0	0	0	0	0	0	0	0	3	0	1	74	1	0	*369*	32	8.43

(e.g. *Anaticinella multicostata*, *Dicarinella* spp., *Globigerinelloides bentonensis*, *Schackoina* spp.) temporarily disappeared across this interval and reappeared within the upper half of the *W. archaeocretacea* Biozone. Assemblages diversified towards the top of the section, where diversity values are similar to those in the Fahdène Formation (Fig. 4).

Assemblages from the lowermost part of the section include common to abundant planispiral (*Globigerinelloides bentonensis*), trochospiral (*Hedbergella delrioensis*, *H. planispira*, *H. simplex*) and biserial forms (*Heterohelix reussi*) (Fig. 5). Right at the base of the *Whiteinella archaeocretacea* Biozone, the abundance of *H. delrioensis* increases up to 67% of the assemblage (metre 7), and minor quantitative peaks in *Thalmanninella brotzeni* and *Whiteinella aprica* are observed (Fig. 5). Assemblages from the lower half of the Bahloul Formation are strongly dominated by *Heterohelix reussi* (up to 78% of the assemblage), whose relative abundance decreases towards the upper half of this formation, where trochospiral taxa (e.g., *W. archaeocretacea*, *W. aprica*, *W. baltica*) become common to abundant. Assemblages from the Kef Formation are similar to those from the upper Bahloul Formation, but they contain higher percentages of triserial (*Guembelitria cenomama*), trochospiral (*Hedbergella delrioensis*) and biserial morphogroups (e.g, *Globoheterohelix paraglobulosa*). A 5 m thick interval in the Kef Formation (metres 37–42) is strongly dominated by *W. aprica*, which is rapidly replaced by *Heterohelix reussi* in the uppermost part of the studied section (Fig. 5).

4.2. Benthic foraminifera

Among benthic foraminifera, calcareous taxa dominate over agglutinated ones. A total of 45 genera and 70 species were recorded throughout the Oued Bahloul section (Appendix 2). *Neobulimina*, *Gavelinella*, *Praebulimina*, *Tappanina*, and *Lenticulina* are the most common genera. *Trochammina*, *Gyroidinoides* and *Laevidentalina* are locally abundant (Fig. 6).

Changes in diversity of benthic foraminiferal assemblages are similar to those of planktic assemblages, showing a decreasing trend from the Fahdéne Formation to the middle part of the Bahloul Formation, with minimum values in metres 10–17, and gradual recovery above this interval towards the top of the section (Fig. 4). Sample 17 (Bahloul Formation) is barren of benthic foraminifera (Fig. 6), and very few specimens were found in samples OB-28, OB-30, OB-37, OB-38 and OB-40; thus the benthic foraminiferal counts are not considered as representative in these samples. While planktic foraminiferal assemblages from the uppermost part of the studied section (upper part of *W. archaeocretacea* Biozone and *H. helvetica* Biozone) reach diversity values similar to those in the Fahdéne Formation, the diversity of benthic foraminifera does not fully recover and is significantly lower at the top of the section.

Benthic foraminiferal assemblages from the lowermost part of the section are diverse and dominated by epifaunal trochospiral forms (e.g., *Gavelinella flandrini*, *Gyroidinoides globosus* and *Gyroidinoides lenticulus*). Spherical (*Trochammina globolaevigata*) and cylindrical tapered morphogroups (*Praebulimina reussi* and *Laevidentalina* spp.) are also common. The relative abundance of *Gavelinella* spp. significantly increases to the top of Pre-Bahloul Member (Fig. 6), and assemblages are clearly dominated by *Gavelinella* spp., *Lenticulina gaultina*, and abundant *Globorotalites* spp. (Fig. 6).

The boundary between the Pre-Bahloul Member and the Bahloul Member (lower part of the *W. archaeocretacea* Biozone) is characterised by an abrupt decrease in the relative abundance of *Gavelinella* and *Lenticulina*, the disappearance of such taxa as *Trochammina* sp., *Globorotalites* spp. and *Lingulogavelinella frankei*, and the temporary disappearance of *Laevidentalina* spp., *Laevidentalina gaultina* and *Lenticulina subgaultina* (Lazarus taxa). This boundary marks a clear change in benthic assemblages, from epifauna-dominated assemblages in the lower part of the section to infauna-dominated

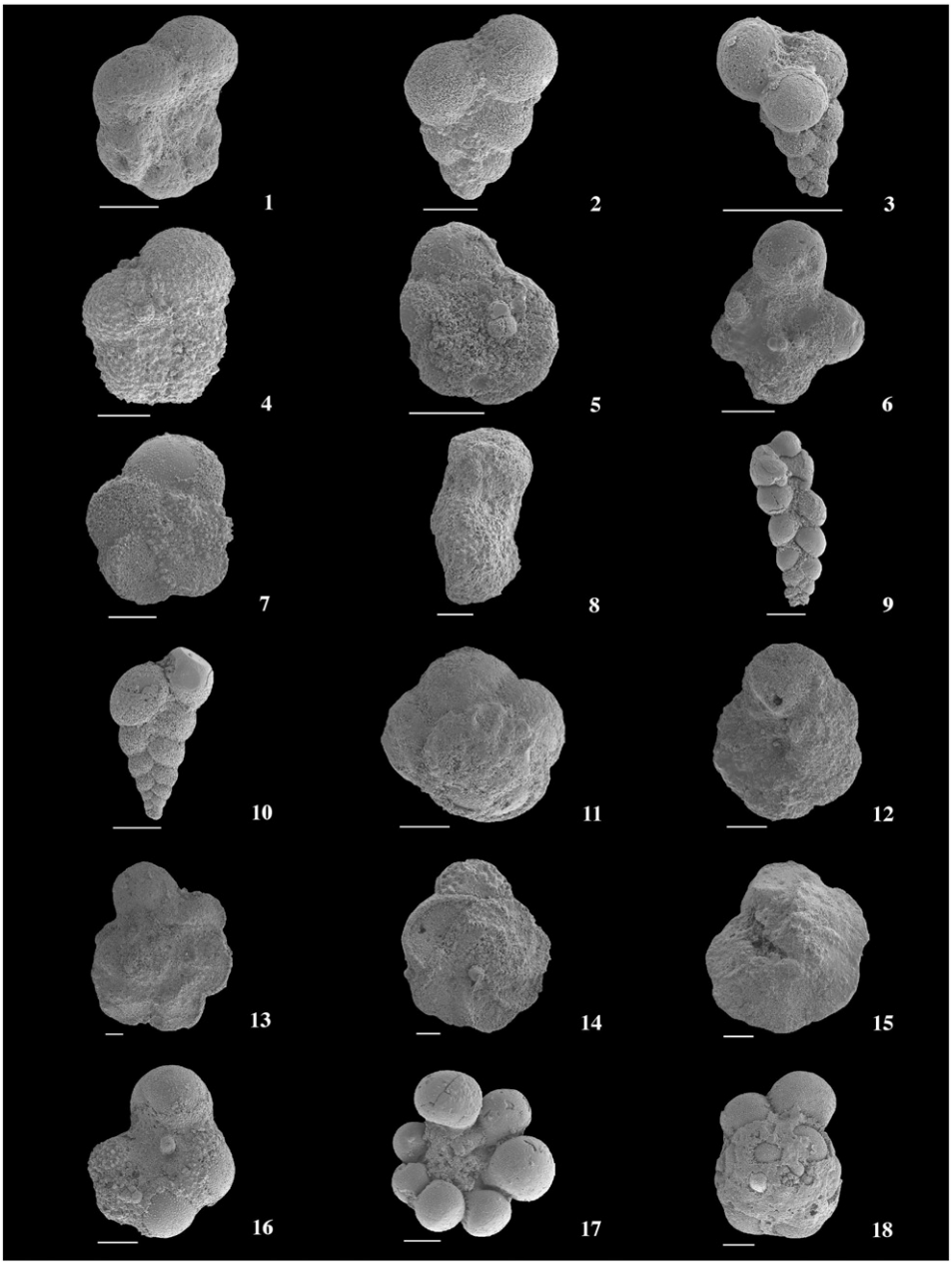

Fig. 2. Planktic foraminiferal species in the Oued Bahloul section: 1 - *Globigerinelloides bentonensis* (OB-3.5). 2 - *Globoheterohelix paraglobulosa* (OB-42). 3 - *Guembelitria cenomana* (OB-24). 4 - *Hedbergella delrioensis* (OB-42). 5- *Hedbergella planispira* (OB-22). 6 - *Hedbergella simplex* (OB-3). 7-8 *Helvetoglobotruncana helvetica* (7: OB-44, 8: OB-35). 9 - *Heterohelix moremani* (OB-13). 10 - *Heterohelix reussi* (OB-22). 11 - *Praeglobotruncana gibba* (OB-3). 12- *Praeglobotruncana stephani* (OB-3.5). 13 - *Rotalipora cushmani* (OB-3). 14- *Rotalipora brotzeni* (OB-3.5). 15 - *Rotalipora greenhornensis* (OB-3.5). 16- *Whiteinella archaeocretacea* (OB-20). 17 - *Whiteinella aprica* (OB-37). 18 *Whiteinella brittonensis* (OB-28). Scale bars: 0.1 mm.

assemblages in the rest of the studied section. Low-diversity assemblages from the lower half of the Bahloul Member are clearly dominated by *Neobulimina albertensis* (up to 81% of the assemblages), with a minor contribution of *Tappanina laciniosa* and *Coryphostoma* spp. The upper part of this member contains more diversified assemblages, with abundant *Neobulimina albertensis* and *T. laciniosa*, common *Laevidentalina* spp., and new taxa such as *Gavelinella rochardensis* and *Bolivina* sp. (Fig. 6).

The lowermost 2.5 m of the *H. helvetica* Biozone are characterised by the disappearance of *Astacolus* spp. and *Dorothia* spp. The Annaba Formation (*H. helvetica* Biozone) contains highly variable percentages of *Neobulimina albertensis* and quantitative peaks of infaunal (*Lenticulina subgaultina*, *Bolivina* spp.) and some epifaunal taxa (*Gavelinella* spp., *Gyroidinoides lenticulus*).

4.3. Geochemistry

4.3.1. Redox proxies

The stratigraphic distribution throughout the succession of the analysed ratios shows three intervals with main changes: a) the base of the *W. archaeocretacea* Biozone, b) the middle part of the *W. archaeocretacea* Biozone, and c) the *W. archaeocretacea*/*H. helvetica* biozone boundary.

The lowermost part of the section (*R. cushmani* Biozone) is characterised by decreasing Co/Al, Ni/Al and Th/Al ratios, followed by a sudden increase in all the studied proxies in the Pre-Bahloul Member (base of *W. archaeocretacea* Biozone, Fig. 7). The Mo_{EF}, $Mo_{aut.}$, U_{EF} and $U_{aut.}$ ratios also increase in the Pre-Bahloul Member, with a dramatic increase in U proxies in the topmost Fahdène Formation (*R. cushmani*/

Table 3
Planktic forms and inferred life style including redox and trophic requirements of planktic foraminifera from Ouled Bahloul section based on Hart and Bailey (1979), Hart (1999), Keller et al. (2001) and Coccioni and Luciani (2004).

Morphology	Genera	Habitat	Mode	Requirements	
				Redox	Trophic
Strongly keeled trochospiral	*Dicarinella*	Intermediate-dweller	Intermediate	Oxygenated	Mesotrophic
	Rotalipora	Intermediate to deep-dweller	Specialist	Well oxygenated	Oligotrophic
	Thalmanninella	Intermediate to deep-dweller	Specialist	Well oxygenated	Oligotrophic
Weakly keeled trochospiral	*Anaticinella*	Intermediate-dweller	Intermediate	Oxygenated	Mesotrophic
	Helvetoglobotruncana	Intermediate to deep-dweller	Intermediate to specialist	Oxygenated to well oxygenated	Mesotrophic to oligotrophic
	Praeglobotruncana	Intermediate-dweller	Intermediate	Oxygenated	Mesotrophic
Unkeeled trochospiral	*Hedbergella*	Surface-dweller	Opportunist	Oxygenated to poorly oxygenated	Eutrophic
	Shackoina	Intermediate-dweller	Intermediate	Oxygenated to poorly oxygenated	Mesotrophic to eutrophic
	Whiteinella	Surface-dweller	Opportunist	Oxygenated to poorly oxygenated	Mesotrophic to eutrophic
Planispiral	*Globigerinelloides*	Surface to intermediate-dweller	Opportunist to Intermediate	Oxygenated to poorly oxygenated	Mesotrophic to eutrophic
Biserial	*Heterohelix*	Surface to intermediate-dweller	Opportunist	Oxygenated to poorly oxygenated	Eutrophic
Triserial	*Guembelitria*	Surface-dweller	Opportunist	Poorly oxygenated	Eutrophic

W. archaeocretacea biozone boundary), immediately preceding the peaks of all other proxies. The U_{EF} values reach 8.08, which is very relevant (Fig. 7). According to Trivobillard et al. (2012), values of elemental enrichment factor >3 are considerable and >10 is considered as a strong enrichment.

An increase in the Cr/Al ratio and in Mo_{EF} and Mo_{aut} values, and a minor increase in Cu/Al, Ni/Al, U_{EF} and U_{aut} are recorded in sample OB-17 (metre 17, middle part of the *W. archaeocretacea* Biozone), which is barren of benthic foraminifera (Fig. 7).

The Th/Al ratio remains constant throughout the rest of the section, while the other proxies increase towards the top of the Bahloul Formation (*W. archaeocretacea*/*H. helvetica* biozone boundary), where new peaks in Co/Al, Cr/Al, Cu/Al, Ni/Al and Mo_{EF} and minor increases in Th/Al, Mo_{aut}., U_{EF} and U_{aut} are observed (Fig. 7). Towards the top of the section (Annaba Member), the selected ratios return to the original values recorded in the lowermost part of the section (Fahdène Formation).

4.3.2. Palaeoproductivity proxies and TOC

In contrast to redox proxies, the selected palaeoproductivity proxies and TOC only show prominent changes in the Pre-Bahloul Formation (base of the *W. archaeocretacea* Biozone; Fig. 8). The U/Al and P/Ti ratios increase coinciding with the first peak in redox proxies, whereas TOC reaches the maximum values (2.8 wt.%) 1 m above the U/Al and P/Ti peaks. TOC values fluctuate throughout the rest of the section but never exceed the high values recorded at the top of the Pre-Bahloul Formation. The Sr/Al ratio and TOC values (2.1 wt.%) are higher in the *W. archaeocretacea*/*H. helvetica* biozone boundary than in the other biozones. Apart from decreased TOC and Sr/Al values in the lower half of the Annaba Member, palaeoproductivity proxies remain relatively stable up to the top of the section.

4.3.3. $\delta^{13}C$ and $\delta^{18}O$

Bulk rock $\delta^{13}C$ values obtained in this study have been compared to previous results by Caron et al. (2006) and Zagrarni et al. (2008), and show similar trends (Fig. 9). A 2‰ increase (from 1.83–3.76‰) in $\delta^{13}C$ is recorded at the transition from the Pre-Bahloul Member to the Bahloul Member (lower part of the *W. archaeocretacea* Biozone). A marked increase in $\delta^{13}C$ values is a typical feature of the OAE2 (e.g. Scholle and Arthur, 1980; Schlanger et al., 1987). $\delta^{13}C$ values remain high throughout most of the *W. archaeocretacea* Biozone (mean value 3.09‰), and decrease in its uppermost 5 m. The $\delta^{13}C$ mean value in the *H. helvetica* Biozone (base of the Annaba Member) is 2.30‰.

The $\delta^{18}O$ values gradually decrease from the Fahdène Formation to the Bahloul Member (from -4.54 to -5.31‰), and remain low (mean value −5.39‰) throughout the rest of the Bahloul Formation, progressively increasing in the Annaba Member (mean value −4.55‰).

5. Palaeoenvironmental interpretation

5.1. Top of the Fahdène Formation and Pre-Bahloul Member

Analysis of redox conditions in the water column and at the seafloor is based on redox-sensitive trace elements (Co, Cr, Cu, Mo, Ni, U, and Th), which tend to co-precipitate with sulfides (mainly pyrite) and are usually not remobilised during diagenesis in the absence of post-depositional replacement of oxidizing agents (Tribovillard et al., 2006). The enrichment in redox sensitive elements (Co/Al, Cr/Al, Cu/Al, U/Al, Th/Al, Mo_{EF}, Mo_{aut}, U_{EF} and U_{aut}) points to depleted oxygen conditions during deposition of the Pre-Bahloul Member (base of the *W. archaeocretacea* Biozone). U-based proxies (U_{EF} = 8.08; Fig. 7) and increased TOC values point to depleted oxygen conditions in the lower part of the water column.

The P/Ti ratio is a commonly used proxy for productivity (Latimer and Filippelli, 2001; Robertson and Filippelli, 2008; Reolid et al., 2012a, b). Increased values are related to higher phosphorous supply to the seafloor derived from biological processes, not from terrigenous components (Latimer and Filippelli, 2001; Flores et al., 2005; Sen et al., 2008). At Oued Bahloul, the increase in P/Ti values at the base of the *W. archaeocretacea* Biozone (Pre-Bahloul Member) indicates an abrupt increase in productivity (Fig. 8). Mort et al. (2007) suggested that the increase in P-accumulation rates coinciding with the OAE2

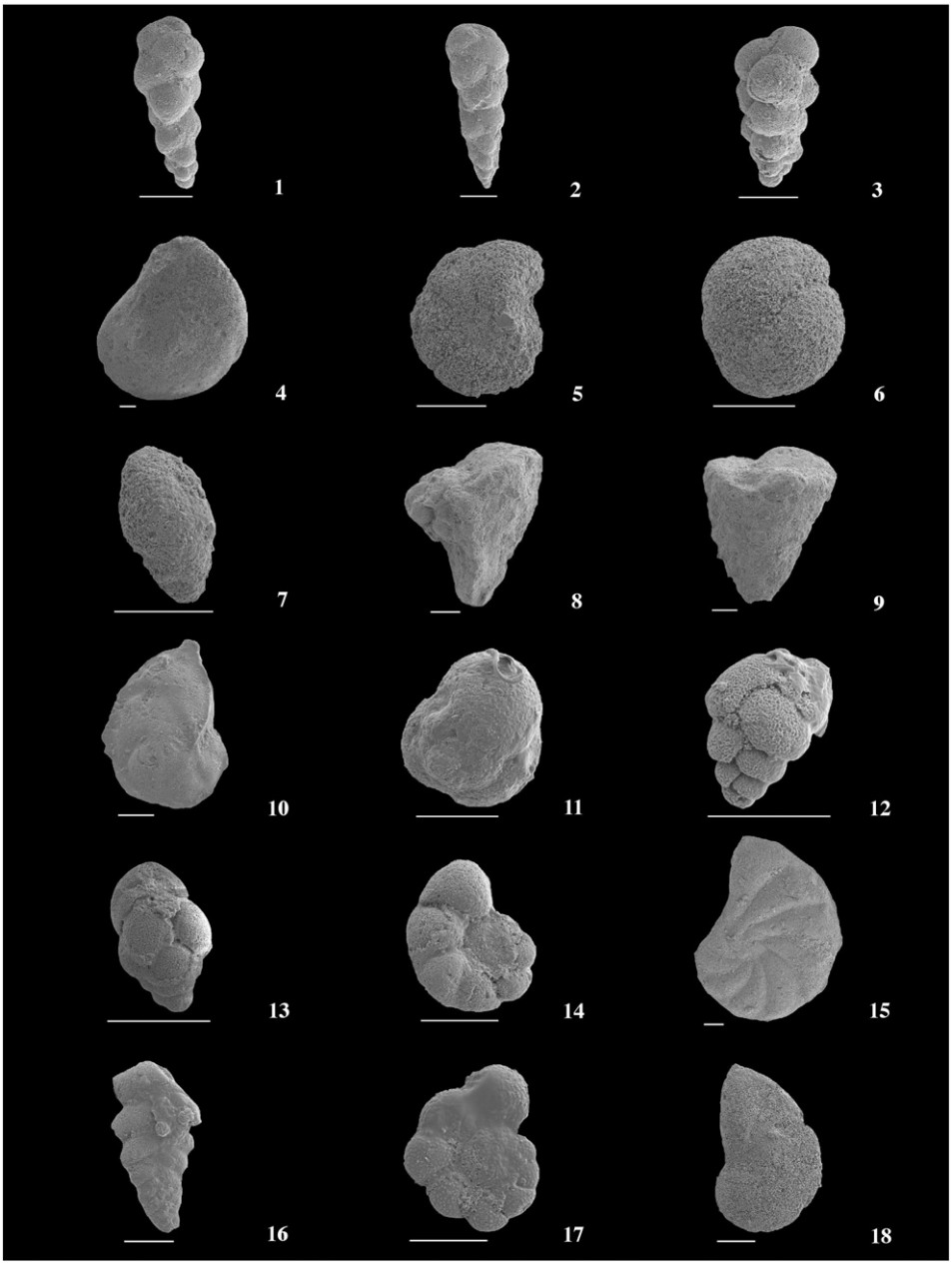

Fig. 3. Benthic foraminiferal species in the Oued Bahloul section: 1 - *Neobulimina albertensis* (OB-10). 2 - *Neobulimina subregularis* (OB-10). 3 - *Praebulimina prolixa* (OB-24). 4 - *Lenticulina gaultina* (OB-2). 5 - *Gyroidinoides lenticulus* (OB-2). 6 - *Gyroidinoides globosus* (OB-2). 7 - *Praebulimina nannina* (OB-2). 8 - *Gaudryina pyramidata* (OB-3). 9 - *Marssonella oxycona* (OB-3). 10 - *Lenticulina* sp (OB-3). 11 - *Trochammina globolaevigata* (OB-3). 12 - *Praebulimina* sp (OB-8). 13 - *Praebulimina reussi* (OB-8). 14 - *Gavelinella rochardensis* (OB-8). 15 - *Planularia advena* (OB-35.5). 16 -*Tappanina laciniosa* (OB-33). 17 - *Gavelinella* cf. *rochardensis* (OB-22). 18 - *Astacolus*? sp. (OB-35). Scale bars: 0.1 mm.

may be related to an overall increase in surface-water productivity. At Oued Bahloul, high P/Ti values coincide with high U/Al and U_{EF} values (Figs. 7 and 8), and point to a productivity increase in the Pre-Bahloul Member. The Sr/Al ratio, which has also been used as a palaeoproductivity proxy (Sun et al., 2008; Reolid et al., 2012a, b), shows a minor increase in the Pre-Bahloul Member (Fig. 8).

This interpretation is compatible with the decreased foraminiferal diversity (both in planktic and benthic assemblages) and with the assemblage turnover at the base of the *W. archaeocretacea* Biozone (Figs. 4–6, 10). Among benthic assemblages, the percentage of *Gavelinella* spp. and *Lenticulina* spp. significantly increases in the Pre-Bahloul Member, and *Globorotalites* shows a minor peak (Fig. 6). *Lenticulina* is regarded as an opportunistic genus that recolonizes the seafloor after redox fluctuations (Tyszka, 1994; Reolid et al., 2008, 2012a). *Gavelinella* spp. is a low-oxygen tolerant genus (Sliter, 1975; Gertsch et al., 2010), and it occurs in shales with high organic matter levels (Holbourn et al., 2001). *Globorotalites* has been observed to peak under stressful conditions at the seafloor after the Cretaceous/Paleogene impact event, mostly related to changes in the type (rather than in the amount) of food supply (Alegret, 2007; Alegret et al., 2012). This assemblage composition, together with the disappearance of some taxa at the *R. cushmani*/*W. archaeocretacea* biozone boundary, indicate dysoxic conditions and a high food flux to the seafloor. The disappearance of *Dorothia*, *Gyroidinoides*, *Laevidentalina*, *Lingulogavelinella*, and *Pyrulinoides* may be related to the dysoxic conditions in the sea-bottom. The boundary between the Pre-Bahloul Member and the Bahloul Member is characterised by the disappearance or abrupt decrease in relative abundance of *Lenticulina*, *Gavelinella* and *Globorotalites*, and by an abrupt increase in low-oxygen tolerant forms such as epifaunal *Neobulimina* (Fig. 6).

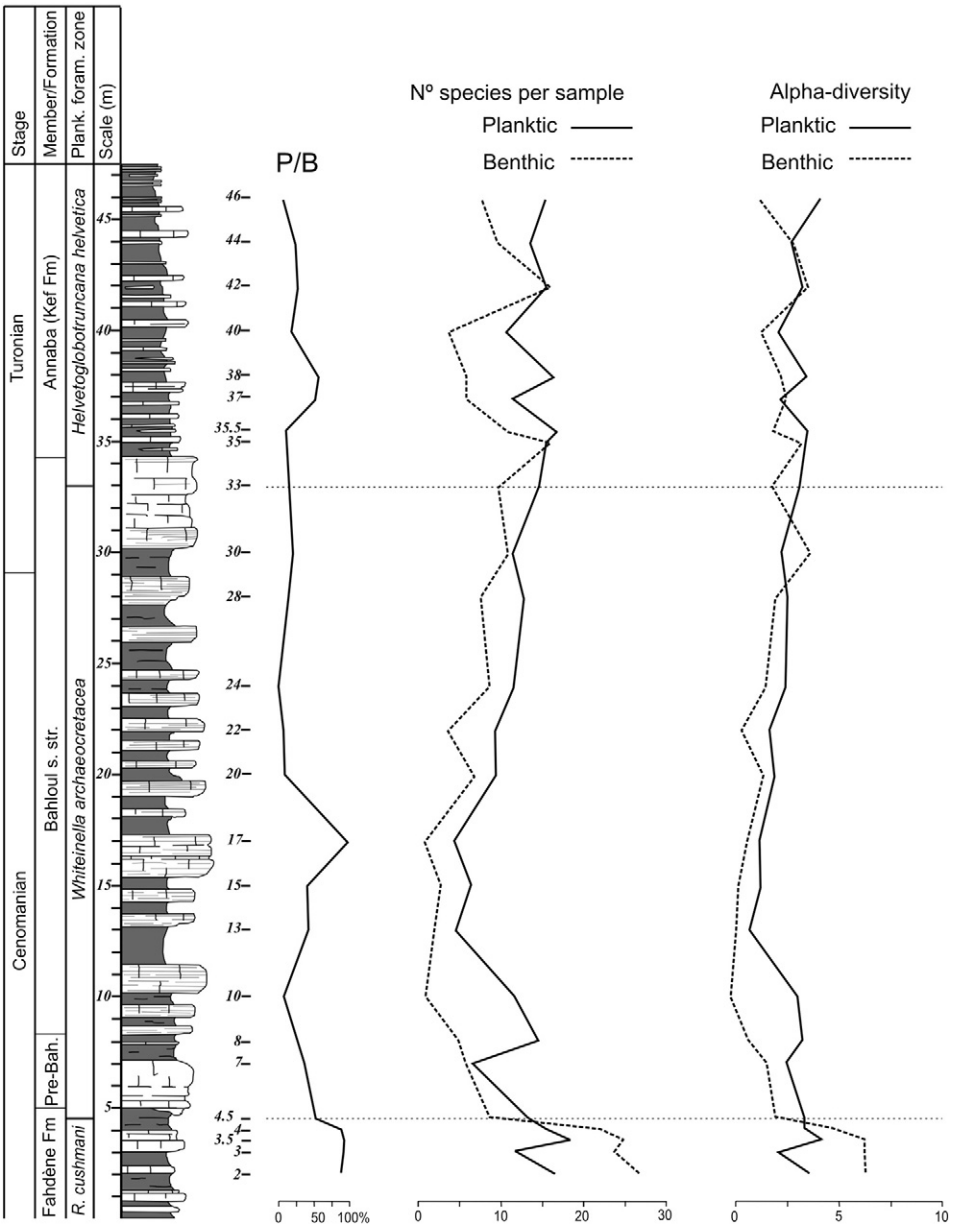

Fig. 4. Stratigraphic distribution of planktic/benthic ratio and diversity of planktic and benthic foraminifera.

The planktic foraminiferal turnover across the Pre-Bahloul Member includes the disappearance of specialist, intermediate to deep-dweller species adapted to oligotrophic environments (*Rotalipora monsalvensis*), along with the temporary disappearance of mesotrophic, intermediate-dwellers (*Praeglobotruncana gibba*, *Dicarinella* spp.). A peak in the relative abundance of the specialist intermediate-dweller *Thalmanninella brotzeni* is recorded at the base of the Pre-Bahloul Member just before its disappearance (Fig. 5). The percentages of the eutrophic, surface-dweller species *Hedbergella delrioensis* (and *Whiteinella aprica* to a minor extent) increase towards the top of the Pre-Bahloul Member, coinciding with the peaks in redox proxies (Figs. 7 and 8), the disappearance of deep-dweller species (*R. cuhsmani*), and the temporary disappearance of surface- and intermediate-dwellers (*Globigerinelloides* spp., *Praeglobotruncana stephani*). These data suggest that the deeper and intermediate layers of the water column were more severely affected than surface waters at the *R. cushmani*-*W. archaeocretacea* biozone transition, as suggested by Coccioni and Luciani (2004). An increase in surface palaeoproductivity is supported by the disappearance of the large keeled *Rotalipora*, a specialist genus probably living at or below the thermocline in oligotrophic conditions (Coccioni and Luciani, 2004; Table 3), and by the increase in relative abundance of small-sized *Hedbergella* and *Heterohelix*, opportunistic taxa adapted to eutrophic conditions (e.g. Hart, 1999; Keller et al., 2001; Table 3). An increase in P content in sections from the Tethys and North Atlantic has been interpreted as indicative of changes in continental input (and nutrient influx) or upwelling intensification during the late Cenomanian (Mort et al., 2007). Monteiro et al. (2012) suggested that a high P content could be sustained by increased chemical weathering and P regeneration from anoxic sediments.

The increase in P/Ti and U/Al in the Pre-Bahloul Member has good stratigraphic correlation with increased redox proxies (Co/Al, Cr/Al, Ni/Al, and Th/Al), and shows a short delay with respect to the increase in TOC values (Figs. 7 and 8). The marine anoxia of the OAE2 is thought to have been related to enhanced biological productivity (e.g. Monteiro et al., 2012; Pogge von Strandmann et al., 2013). Uranium and organic matter in the sediment are related, as uranium may form a complex

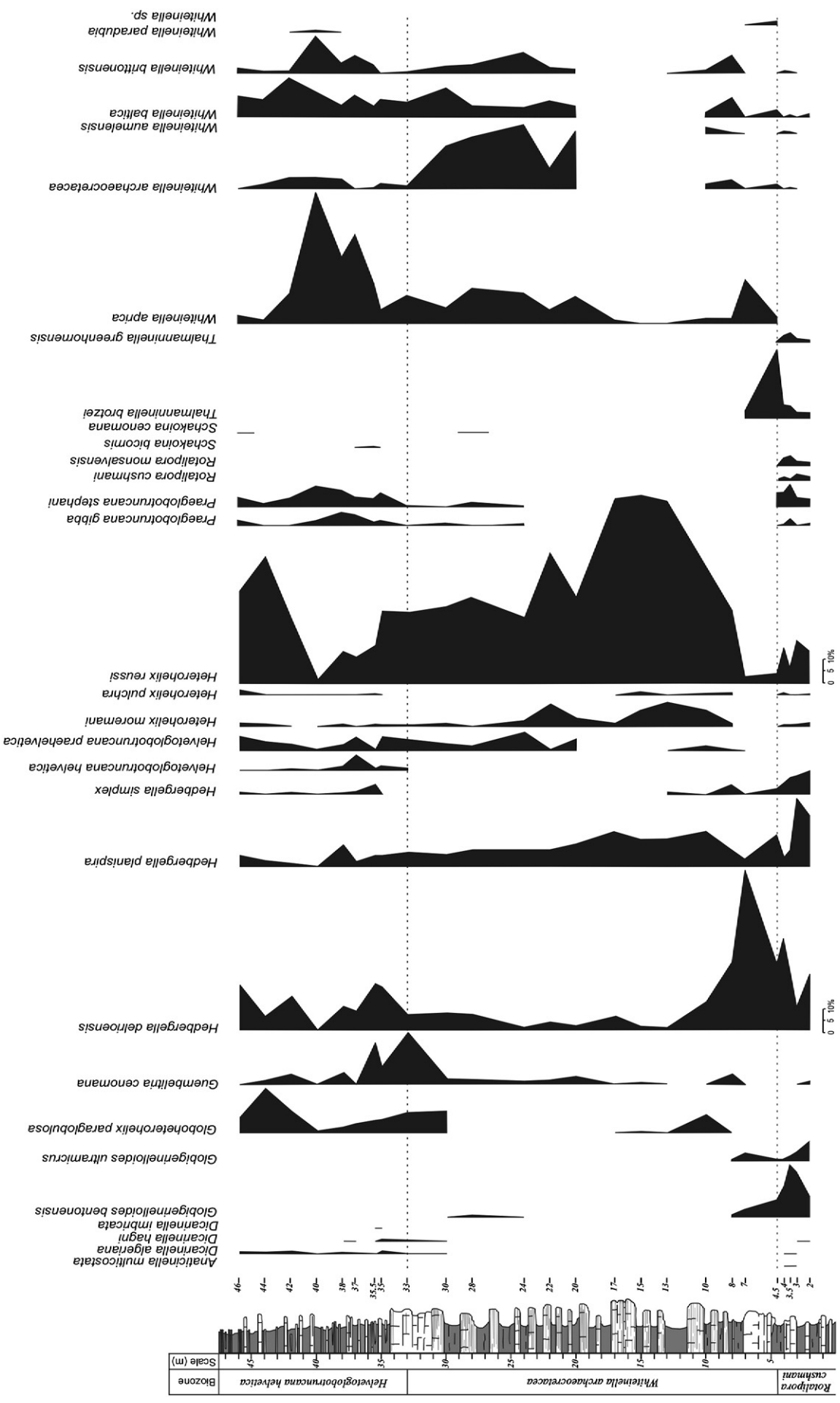

Fig. 5. Stratigraphic distribution of planktic foraminiferal assemblages.

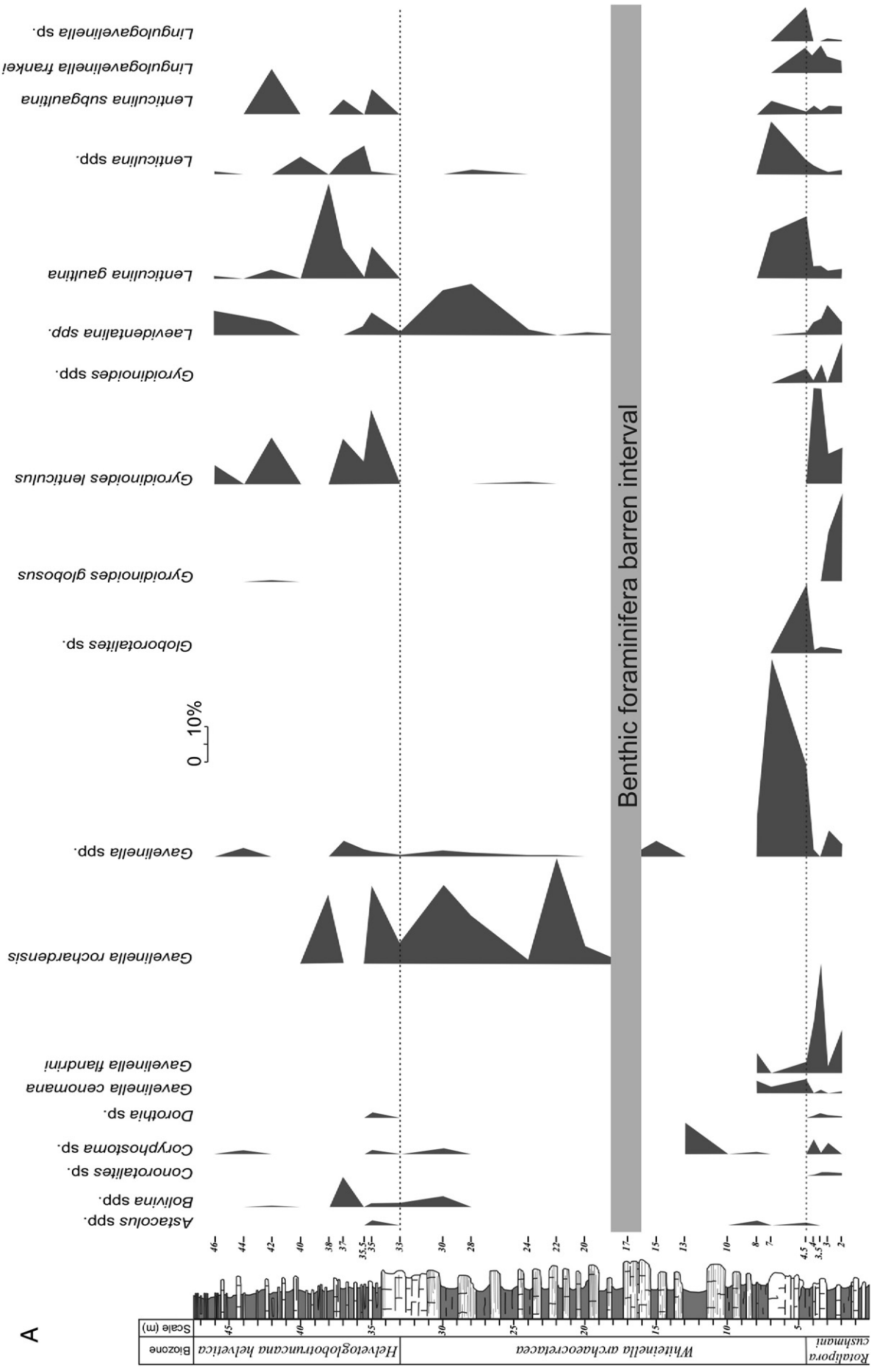

Fig. 6. Stratigraphic distribution of benthic foraminiferal assemblages.

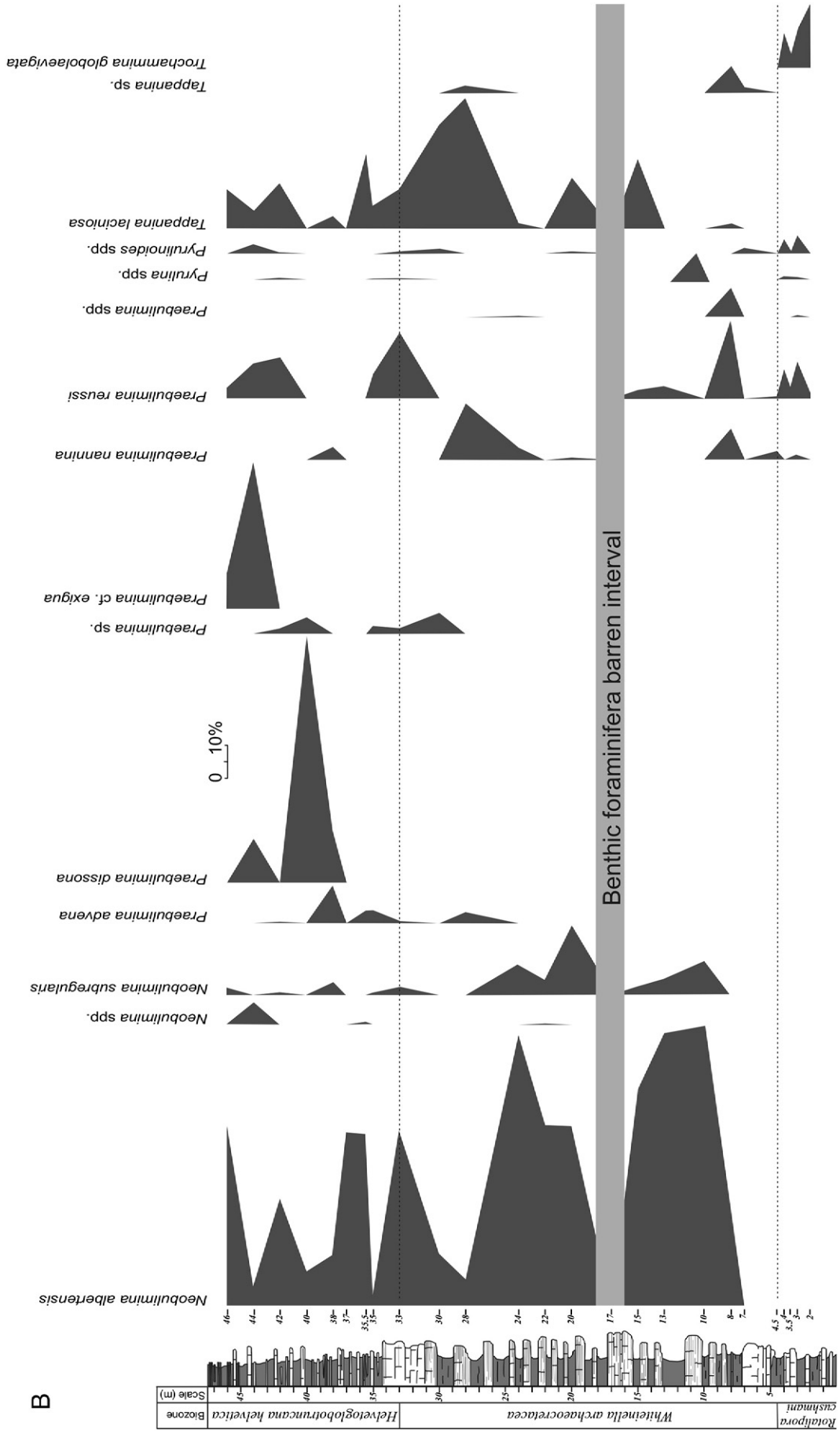
B
Scale (m)
Biozone
Rotalipora cushmani
Whiteinella archaeocretacea
Helvetoglobotruncana helvetica
Neobulimina albertensis
Neobulimina spp.
Neobulimina subregularis
Praebulimina advena
Praebulimina dissona
0 10%
Praebulimina sp.
Praebulimina cf. exigua
Praebulimina nanina
Praebulimina reussi
Praebulimina spp.
Pyrulina spp.
Pyrulinoides spp.
Tappanina lacinosa
Tappanina sp.
Trochammina globolaevigata
Benthic foraminifera barren interval

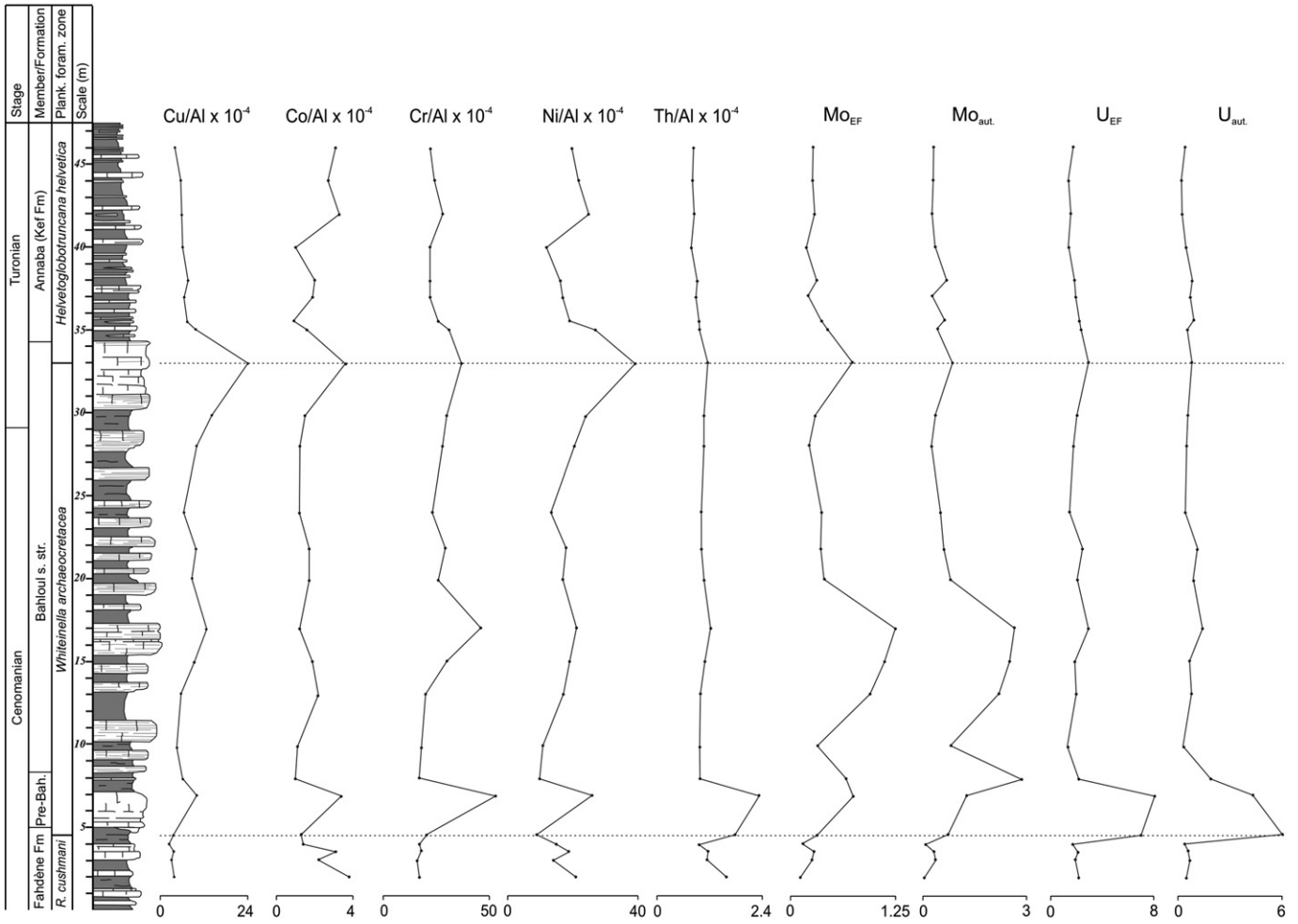

Fig. 7. Stratigraphic fluctuations of geochemical redox proxies and U- and Mo-based proxies (enrichment factor and authigenic content).

with dissolved fulvic acid in hemipelagic sediments (Nagao and Nakashima, 1992). In this sense, high values for U/Al, U_{EF} and U_{aut} are congruent with the high values of P/Ti.

In open-ocean systems with suboxic bottom waters, U_{aut} enrichment is greater than that of Mo_{aut} because U_{aut} accumulation begins at the Fe(II)-Fe(III) redox boundary (Zhou et al., 2012), while Mo_{aut} accumulation becomes more important as waters become euxinic. Higher values of U_{aut} recorded in the Pre-Bahloul Member are congruent with oxygen-depleted conditions not only at the sea-bottom waters but also in the deeper layers of the water column (Fig. 10), where deep dwellers such as *Rotalipora* inhabited. The relative abundance of surface dwellers such as *Hedbergella delrioensis* increased in the Pre-Bahloul Member.

5.2. Bahloul s. str. Member

Two intervals with significant peaks in redox proxies are recorded within the Bahloul Member (Fig. 7). The first one is located in the middle part of this unit (sample OB-17), and the second one is located towards its top, at the *W. archaeocretacea*/H. *helvetica* Biozone boundary (Fig. 7). Some redox proxies, such as Th/Al, U_{EF} and U_{aut}, do not show any significant changes across this interval.

In the lower half of the Bahloul Member (previous to sample OB-17), the amount of dissolved oxygen in the sea-bottom waters is interpreted to have been even lower than in the underlying Pre-Bahloul Member (Fig. 10), as inferred from the disappearance of several benthic foraminiferal taxa and from the very low-diversity assemblages (Figs. 2 and 6), which are dominated by low-oxygen tolerant forms such as *Neobulimina* (Gertsch et al., 2010), *Praebulimina*, *Coryphostoma* and *Tappanina* spp. (incl. *T. laciniosa*). The clear dominance of *Neobulimina* and *Praebulimina* immediately above the extinction interval suggests that they may have behaved as disaster species, as suggested by Peryt and Lamolda (1996). According to these authors, disaster taxa evolved during the late, most stressful phases of an extinction interval, and persisted during the survival and recovery intervals. Species of *Coryphostoma* have small, tapered tests with abundant pores, and are common in dysaerobic environments (e.g., Leutenegger and Hansen, 1979; Bernhard, 1986). *Coryphostoma* is a common genus in low-oxygen environments during the early Danian (Coccioni et al., 1993; Alegret, 2007), and *Tappanina laciniosa* is a biserial, infaunal species that has been reported from dysoxic facies in highly eutrophic environments (e.g. Eicher and Worstell, 1970; Gustafsson et al., 2003; Friedrich and Erbacher, 2006). Moreover, the dominance of infaunal taxa in the Bahloul Member and in the Annaba Member supports the interpretation of low oxygen conditions at the seafloor (Jorissen et al., 1995).

The decreased abundance of the surface-dweller *Hedbergella delrioensis* at the base of the Bahloul Member (Fig. 5) points to oxygen-depleted eutrophic surface waters, while low-oxygen conditions only affected deep and intermediate waters in the underlying Pre-Bahloul Member. Only *Heterohelix reussi* —opportunistic taxon adapted to eutrophic conditions – proliferates in the lower part of Bahloul Member in a context of decreasing diversity of planktic foraminiferal assemblages.

Relatively higher TOC values (mean 1.42 wt.%) and high $\delta^{13}C$ are recorded in the Bahloul Member (Fig. 8), suggesting higher productivity

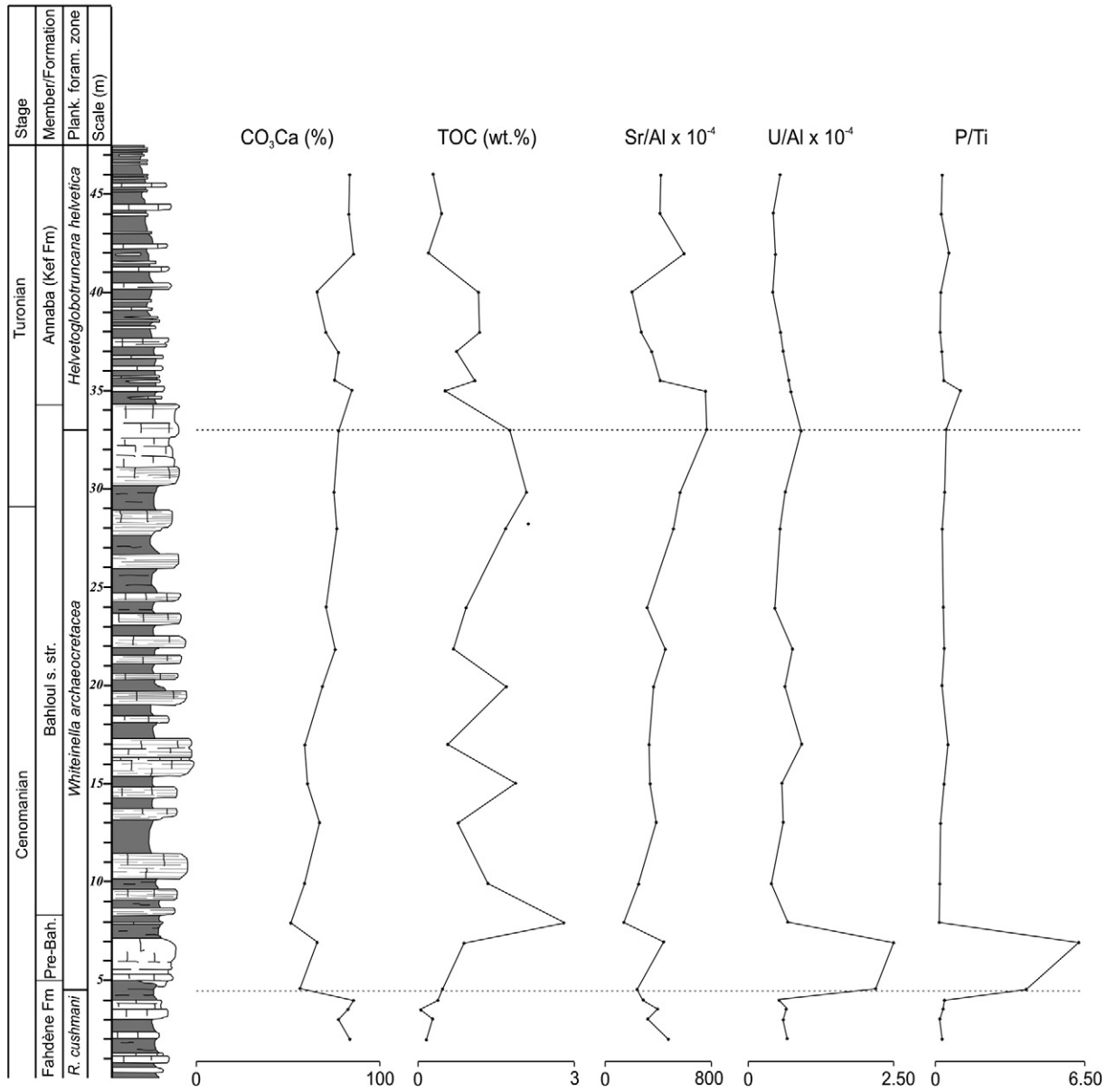

Fig. 8. Stratigraphic fluctuations of CO_3Ca content, TOC and geochemical palaeoproductivity proxies.

than in the other units and high accumulation of organic matter derived from surface primary productivity (Schlanger and Jenkyns, 1976; Arthur et al., 1990; Ingall et al., 1993; Van Cappellen and Ingall, 1994; Mort et al., 2007). TOC values have been used as an indirect palaeoproductivity proxy by various authors (e.g., Calvert and Fontugne, 2001; Gupta and Kawahata, 2006; Plewa et al., 2006; Su et al., 2008; Reolid et al., 2012a) when TOC is related to phytodetritus associated with phytoplankton or dinoflagellate remains. Nevertheless, because high TOC values may result from low bottom-water ventilation and oxygen depletion, they are not necessarily related to high surface productivity. According to Tribovillard et al. (2006), the TOC is generally proportional to surface-water productivity and constitutes a useful palaeoproductivity proxy in spite of certain complications attributable to efficient organic recycling, export productivity, delivery to the sediment-water interface and final burial. The maximum TOC values (2.82 wt.%) are recorded at the base of this unit (Fig. 8), coeval with high percentages of *Heterohelix reussi*, *Heterohelix moremani* and *Hedbergella planispira* (Fig. 5), which are thought to be indicative of eutrophic environments (Table 3). These results are compatible with the analyses of organic matter carried out by Farrimond et al. (1990), who reported abundant algal-derived biological markers across the Cenomanian-Turonian transition at Oued Bahloul, suggesting high surface productivity. High TOC values are also correlated to high percentages of *Neobulimina* and other buliminids (Fig. 6), which are considered to be indicators of high-food and/or low oxygenation at the seafloor in the modern oceans (e.g., Fontanier et al., 2002; Gooday, 2003). The dominance of buliminids is also compatible with the proposed conditions, given that high proportions of buliminids indicate eutrophic conditions (Sprong et al., 2013). These results point to a high export productivity and poor oxygenation at the sea-bottom waters during deposition of the lower part of the Bahloul Member; and combined with the high TOC and $\delta^{13}C$ values (Figs. 8 and 9), they suggest a major climatic and palaeoceanographic perturbation in a transgressive context (e.g. Zagrarni et al., 2008). In addition, Caron et al. (1999) and Soua et al. (2011) documented the proliferation of radiolarians (mainly Nassellarian) and diatoms at the base of the *Whiteinella archaeocretacea* Biozone (from the uppermost Pre-Bahloul Member), in coincidence with an increased abundance of *Heterohelix* during the deposition of

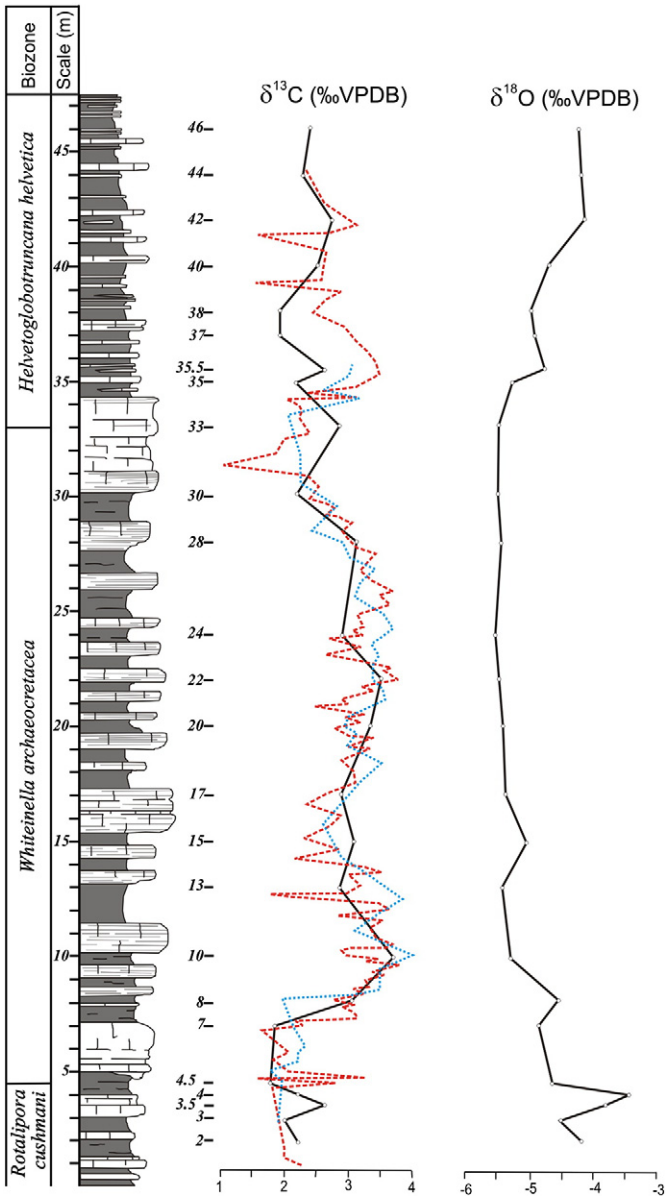

Fig. 9. Stratigraphic fluctuations of $\delta^{13}C$ and $\delta^{18}O$ and comparison with previous $\delta^{13}C$ curves of Caron et al. (2006) (dashed line) and Zagrarni et al. (2008) (dotted line).

dark laminated limestones. These authors interpreted the proliferation of radiolarians as indicative of renewal of nutrient-rich oceanic waters and increase in water depth.

An increase in Mo_{EF} and Mo_{aut}, and a minor increase in Cu/Al, Cr/Al and Ni/Al are observed in bed OB-17 (Fig. 7). High Mo_{EF} and Mo_{aut} values require the presence of H_2S (euxinic conditions) (Trivobillard et al., 2012; Zhou et al., 2012). The gradual increase in Mo_{EF} and Mo_{aut} across the lower half of the studied section indicates a progressive decrease in oxygen availability towards euxinic conditions. Other authors have reported euxinic conditions from the OAE2 (e.g. Wang et al., 2001; Scopelliti et al., 2004). The progressive accentuation of oxygen-depleted conditions from the Pre-Bahloul Member towards the lower half of the Bahloul Member is compatible with the disappearance of benthic taxa that flourished at the beginning of the suboxic conditions (e.g., *Lenticulina*, *Gavelinella*, *Globorotalites*), and with the proliferation of the disaster genus *Neobulimina* (low oxygen tolerant form, Friedrich et al., 2009), which has been documented from other sections during the Cenomanian–Turonian event (e.g. Gebhardt et al., 2004) (Fig. 10). Finally, the interpretation of anoxia/euxinia is compatible with the lack of benthic foraminifera and very low diversity of planktic assemblages in sample OB-17. The bed OB-17 represents a benthic barren level. Unfavorable conditions also affected the water column during this interval, as inferred from the dramatic decrease in the percentage of the opportunistic surface dweller *Hedbergella delrioensis* and the increase in opportunistic surface to intermediate dwellers (*Heterohelix* spp.). The highest relative abundances of heterohelicids (*H. reussi*) occur in OB-17 (Fig. 5), where maximum values of Mo_{EF} and Mo_{aut} are recorded (Fig. 7). *Heterohelix* has been interpreted as a low-oxygen tolerant genus that bloomed in stratified open marine settings with a well-developed oxygen minimum zone (e.g. Leckie et al., 1998; Premoli Silva and Sliter, 1999; Keller et al., 2001; Keller and Pardo, 2004).

Redox proxies indicate the return to normal oxygen conditions across the upper half of the Bahloul Member (Fig. 10), but the palaeoenvironmental perturbation induced slow recovery of the foraminiferal assemblages, as reflected by the dominance of the opportunistic *Heterohelix* and *Whiteinella* in intermediate and surface waters, respectively. Diversity of benthic assemblages slightly increases through this interval, and assemblages are dominated by buliminids (*Neobulimina* and *Praebulimina*), with higher percentages of *Gavelinella rochardensis*, *Laevidentalina* and *T. laciniosa* towards the upper part of the Bahloul Formation. The species *T. laciniosa* and the genera *Gavelinella*, *Neobulimina* and *Praebulimina* have been reported from dysoxic facies in highly eutrophic environments and high organic-matter fluxes (e.g. Eicher and Worstell, 1970; Coccioni et al., 1993; Gustafsson et al., 2003; Gebhardt et al., 2004; Friedrich and Erbacher, 2006; Friedrich et al., 2009). This assemblage suggests that the repopulation phase at the seafloor occurred in the upper half of the Bahloul Formation. Among planktic foraminifera, the opportunistic surface dweller *Whiteinella* proliferated in this interval, together with the intermediate dweller *H. reussi*, as previously reported from the Tethys area (Coccioni and Luciani, 2004). Non-opportunist forms including *Praeglobotruncana* and *Dicarinella* are recorded in the upper part of the *W. archaeocretacea* Biozone, whereas deep dweller specialists as *Rotalipora* are definitively extinct and there are no genera occupying this ecologic niche.

A positive peak in redox proxies (Mo_{EF}, Cu/Al, Co/Al, Cr/Al, Ni/Al ratios) and a minor increase in some palaeoproductivity proxies have been recorded at the *W. archaeocretacea*/*H. helvetica* biozone boundary (sample OB-33), coinciding with an increase in the percentage of buliminids and *Guembelitria cenomana*. *Guembelitria* is interpreted as an opportunist surface dweller adapted to poorly oxygenated, eutrophic waters (Table 3) or to variable salinity and nutrient levels (Keller and Pardo, 2004). The obtained data indicate high productivity and low-oxygen conditions both in surface waters and at the seafloor towards the top of the *W. archaeocretacea* Biozone. According to Soua et al. (2011), the composition of radiolarian assemblages also experiments a turnover related to low-oxygen conditions with a drastic decrease of nassellarians and an abundance and diversification of spumellarians.

5.3. Base of the Kef Formation

A progressive increase in the diversity of planktic assemblages, together with the co-occurrence of surface and intermediate-to-deep dwellers indicates partial recovery of the assemblages at the beginning of the *H. helvetica* Biozone. The most common taxa (*Whiteinella*, *Heterohelix*, *Hedbergella*) are indicative of eutrophic, oxygenated to poorly oxygenated surface and intermediate waters. Deep dwellers such as the intermediate to specialist *Helvetoglobotruncana* (Table 3) make only a minor contribution to the assemblages. Just after the last suboxic pulse of the top of Bahloul Member (level OB-33), *Whiteinella* proliferates again in the assemblage as a rapid response to improved conditions.

In benthic microhabitats, the beginning of the *H. helvetica* Biozone is marked by an increase in relative abundance of *Gyroidinoides*,

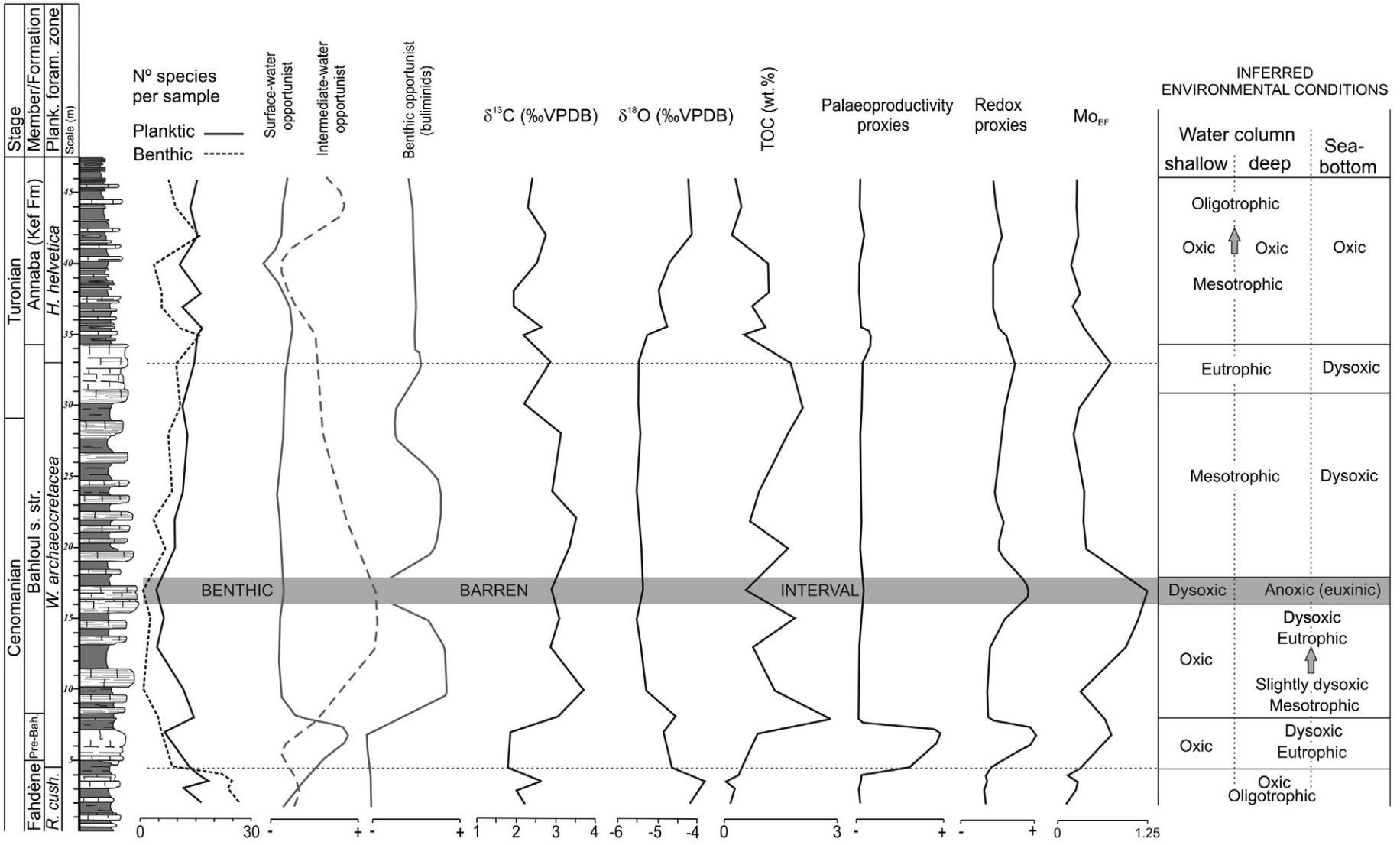

Fig. 10. Evolution of trophic conditions, productivity and oxygenation in the water column and the seafloor (sea-bottom waters) inferred from foraminiferal assemblages and geochemical proxies.

Lenticulina and *Planularia*, and a decrease in *Tappanina* and *Gavelinella*. Diversity of the benthic assemblages remains low, and the dominance of buliminids (*Praebulimina* and *Neobulimina*) indicates a high food supply or low-oxygen conditions at the seafloor (Jorissen et al., 1995; Widmark and Speijer, 1997; Fontanier et al., 2002).

6. Climatic and palaeoceanographic changes across the Cenomanian–Turonian boundary

Analyses of $\delta^{18}O$ in bulk rock show a ~1.5‰ decrease from the base of the section towards the Bahoul Member, followed by a gradual recovery above this unit (Fig. 9). Assuming these results have not been strongly altered by diagenesis, we infer significantly warmer (~6 °C) temperatures during deposition of the organic rich facies of the Bahoul Member (*W. archaeocretacea* Biozone), coeval with the disappearance of specialist planktic foraminifera (e.g. *Rotalipora*) and with the proliferation of opportunistic, eutrophic forms such as *Heterohelix* and *Hedbergella*. These results suggest a narrow link between the development of the anoxic event and eutrophic conditions with changes in the ocean-atmosphere system. Some authors have identified a short term cooling during the OAE2 (e.g. Jarvis et al., 2011; Gavrilov et al., 2013; Zheng et al., 2013), which we were not able to recognize in our record from Oued Bahloul at the present resolution.

In the transgressive context of the Cenomanian–Turonian boundary (e.g. Zagrarni et al., 2008), the enhanced fertility resulting in high primary productivity and eutrophication was favored by nutrient inputs by leaching from flooded shelves (Erbacher et al., 2001) or enhanced continental supply of nutrients (Föllmi, 1995; Handoh and Lenton, 2003). According to Wagner et al. (2007), the warm humid climate contributes to an intensified hydrological cycle and enhanced export of nutrient-rich weathered material from land to the ocean, as also suggested for the Paleocene-Eocene Thermal Maximum (see refs. in Arreguín-Rodríguez et al., 2014). For the end of Cenomanian, another hypothesis was developed by Caron et al. (1999): the alternation of climatic fluctuations, with evaporation/precipitation in low latitude areas and the formation of dense, hypersaline sea waters.

Calcareous nannofossil turnover has been interpreted in terms of enhanced fertility and increased temperatures, pointing to an eutrophication event (Erba, 2004; Hardas and Mutterlose, 2007). P-cycling models for Cretaceous Anoxic Events, however, indicate that enhanced primary productivity is not enough for producing anoxic conditions in the bottom waters if water circulation exists (Tsandev and Slomp, 2009). According to these authors, the global ocean has to be sufficiently stagnant (low mixing) to allow the system to achieve oxygen depletion in the deep sea. In general, the thermohaline circulation during the Cretaceous is believed to have been slower due to reduced thermal gradients between the tropics and poles (e.g. Schlanger and Jenkyns, 1976; Fischer and Arthur, 1977), and the wider extension of continental shelves (e.g. Bjerrum et al., 2006). In this context, increased P supply from flooded shelves and weathered continental areas may have triggered enhanced primary production and anoxia in a stagnant ocean. In the Oued Bahloul section, a significant increase in P has been observed in the Pre-Bahloul Member coeval with high dominance of *Hedbergella* and the extinction of *Rotalipora*. The progressive decrease in oxygenation of bottom- and deep-waters towards anoxic conditions in the Bahloul Member (metre 17, OB-17) represents the most stressing conditions for the foraminiferal assemblages, with the disappearance of benthic foraminifera, the expansion of the oxygen minimum zone coincident with maximum values of *Heterohelix*, and probably euxinic conditions in the low water column as indicated by increased Mo_{EF} and $Mo_{aut.}$

7. Conclusions

The integrated analysis of planktic and benthic foraminiferal assemblages, geochemical proxies, TOC and $\delta^{13}C$ and $\delta^{18}O$ from the classic locality of the Oued Bahloul section allowed us to interpret: (a) the redox and palaeoproductivity fluctuations related to the C/T boundary, and (b) the ecostratigraphic changes of foraminiferal associations across the OAE2.

Significant changes were recorded across the *R. cushmani*/*W. archaeocretacea* boundary, and planktic and benthic foraminiferal diversity decreased. The disappearance of the planktic genera *Rotalipora*, *Praeglobotruncana*, *Globigerinelloides* and *Thalmanninella*, and the occurrence of the opportunist genus *Hedbergella*, together with the proliferation of buliminids and the increase in palaeoproductivity proxies (P/Ti, U/Al, Sr/Al), indicate eutrophic conditions both in the water column and at the seafloor. The abundance of low-oxygen tolerant genera of benthic foraminifera at the base of *W. archaeocretacea* Biozone is compatible with the enrichment in redox proxies indicating dysoxic conditions in sediment pore water. Deep waters were also oxygen-depleted, as deduced from higher values of U_{aut} than Mo_{aut}, favouring the disappearance of *Rotalipora* and *Globigerinelloides* and the proliferation of surface-dweller *Hedbergella*. The maximum TOC values registered in the lower part of the *W. archaeocretacea* Biozone indicate an abrupt increase in organic matter coeval with an increase in palaeoproductivity and redox proxies.

The persistence of the poorly oxygenated conditions in the *W. archaeocretacea* Biozone probably produced euxinic conditions, as indicated by high Mo_{EF} and Mo_{aut} values, minimum diversity and the local disappearance of benthic forms. The decrease in abundance of opportunist surface dwellers (*Hedbergella*) and the increase in opportunist intermediate dwellers (heterohelicids), together with maximum values of Mo_{EF} and Mo_{aut}, indicate stressed conditions and stratified open marine settings with a well-developed oxygen minimum zone.

The redox proxies indicate a return to normal oxygen conditions in the upper part of the *W. archaeocretacea* Biozone, with a slow recovery of foraminiferal assemblages. The genus *Whiteinella*, characteristic of mesotrophic environments, becomes more abundant upward in the section. The subsequent colonization of the bottom after the anoxic event was produced by *Praebulimina* (disaster genus), *Gavelinella*, *Neobulimina* and *Tappanina*. These genera are low-oxygen tolerant and related to high organic matter fluxes, thus representing the repopulation episode of the bottom after the benthic barren interval.

The *W. archaeocretacea*/*H. helvetica* biozone boundary is characterized by increasing values of redox proxies, coeval with a new peak of *Praebulimina*, a decrease in *Whiteinella* and the record of opportunist *Guembelitria*.

The beginning of the *H. helvetica* Biozone indicates a partial recovery of the planktic foraminiferal assemblage due to a persistent dominance of opportunists (*Whiteinella* and *Hedbergella* in surface waters, and *Heterohelix* in intermediate waters). In benthic microhabitats, the beginning of the *H. helvetica* Biozone is marked by an increase in relative abundance of *Neobulimina*, *Lenticulina*, and *Gyroidinoides*, and a decrease in *Tappanina*.

Temperature changes and palaeoceanographic reorganization have been inferred across the OAE2. This entailed a low mixing of surface and deep waters (poor ocean ventilation) and enhanced primary productivity related to global warming, increasing continental weathering and nutrient input to the ocean. The expansion of the oxygen minimum zone and the eutrophication led to a reduced diversity of foraminifera and the planktic foraminiferal shift, showing a dominance of genera with low-oxygen tolerance typical of high mesotrophic to eutrophic conditions.

Acknowledgements

We thank Dalila Zaghbib-Turki (Université de Tunis El Manar) and Mohamed Soua (Entreprise Tunisienne d'Activités Pétrolières), who helped us sample the Oued Bahloul section. This research was supported by Projects RYC-2009-04316 (Ramón y Cajal Program, Ministerio de Ciencia e Innovación + FSE), Project CGL2012-33281 (Secretaría de

Estado de I + D + I, Spain), P11-RNM-7408 (Junta de Andalucía), and Projects CGL2011-23077 and CGL2011-22912 of the Spanish Ministry of Science and Technology (FEDER funds) and the consolidated group E05 funded by the Government of Aragon. Sánchez-Quiñónez, C.A. thanks the Fundación Carolina (Spain) for a grant for supporting his research stay at the Universidad de Zaragoza. We thank the editor Finn Surlyk and the reviewers Michèle Caron (Universität Freiburg) and an anonymous reviewer for comments. The authors thank Jean Louise Sanders for improving English language.

Appendix 1. Planktic foraminiferal species

Anaticinella multiloculata (Morrow, 1934)
Dicarinella algeriana (Caron, 1966)
Dicarinella hagni (Scheibnerova, 1962)
Dicarinella imbricata (Mornod, 1950)
Globigerinelloides bentonensis (Morrow, 1934)
Globigerinelloides ultramicrus (Subbotina, 1949)
Globoheterohelix paraglobulosa Georgescu and Huber, 2009
Guembelitria cenomana (Keller, 1935)
Hedbergella delrioensis (Carsey, 1926)
Hedbergella planispira (Tappan, 1940)
Hedbergella simplex (Morrow, 1934)
Helvetoglobotruncana helvetica (Bolli, 1945)
Helvetoglobotruncana praehelvetica (Trujillo, 1960)
Heterohelix moremani (Cushman, 1938)
Heterohelix pulchra (Brotzen, 1936)
Heterohelix reussi (Cushman, 1938)
Praeglobotruncana gibba Klaus, 1960
Praeglobotruncana stephani (Gandolfi, 1942)
Rotalipora cushmani (Morrow, 1934)
Rotalipora monsalvensis (Mornod, 1950)
Shackoina bicornis (Reichel, 1948)
Schackoina cenomana (Shacko, 1897)
Thalmanninella brotzeni (Sigal, 1948)
Thalmanninella greenhornensis (Morrow, 1934)
Whiteinella aprica (Loeblich and Tappan, 1961)
Whiteinella archaeocretacea Pesaggno, 1967
Whiteinella aumalensis (Sigal, 1952)
Whiteinella baltica Douglas and Rankin, 1969
Whiteinella brittonensis (Loeblich and Tappan, 1961)
Whiteinella paradubia (Sigal, 1952)
Whiteinella sp.

Appendix 2. Benthic foraminiferal species

Ammodiscus spp.
Arenobulimina spp.
Astacolus spp.
Bathysiphon spp.
Bigenerina sp.
Bolivina sp.
Bolivinopsis sp.
Brunsvigella thoerensis (Bartenstein and Brand, 1951)
Charltonina australis Scheibnerová, 1978
Charltonina sp.
Conorotalites sp.
Coryphostoma spp.
Dorothia pupa (Reuss, 1860)
Dorothia spp.
Frondicularia sp.
Gaudryina pyramidata Cushman, 1926
Gaudryina spp.
Gavelinella barremiana Bettenstaedt, 1952
Gavelinella cenomanica (Brotzen, 1945)
Gavelinella flandrini Moullade. 1960
Gavelinella intermedia (Berthelin, 1880)
Gavelinella rochardensis Beckmann, 1991
Gavelinella spp.
Glandulina sp.
Globorotalites sp.
Globulina spp.
Gyroidinoides beisseli (White, 1928)
Gyroidinoides globosus (Hagenow, 1842)
Gyroidinoides lenticulus (Reuss, 1845)
Gyroidinoides spp.
Gyroidinoides subglobosus Dailey, 1970
Laevidentalina spp.
Lagena spp.
Lenticulina gaultina (Berthelin, 1880)
Lenticulina spp.
Lenticulina subgaultina Bartenstein, 1962
Lingulina sp.
Lingulina taylorana Cushman, 1938
Lingulogavelinella frankei (Bykova, 1953)
Lingulogavelinella sp.
Marssonella oxycona (Reuss, 1860)
Neobulimina albertensis (Stelck and Wall, 1954)
Neobulimina irregularis Cushman and Parker, 1936
Neobulimina spp.
Neobulimina subregularis (de Klasz, Magné and Rérat, 1963)
Neoflabellina sp.
Palmula sp.
Planularia advena Cushman and Jarvis, 1932
Planularia dissona Plummer, 1931
Planularia sp.
Praebulimina cf. *exigua* Cushman and Parker, 1935
Praebulimina nannina (Tappan, 1940)
Praebulimina reussi (Morrow, 1934)
Praebulimina spp.
Pyrulina spp.
Pyrulinoides spp.
Quadrimorphina sp.
Quasispiroplectammina spp.
Ramulina spp.
Reophax sp.
Repmanina charoides (Jones and Parker, 1860)
Saracenaria sp.
Spiroplectammina sp.
Stensioeina exsculpta (Reuss, 1860)
Tappanina laciniosa Eicher and Worstell, 1970
Tappanina sp.
Textularia sp.
Trochammina globolaevigata Beckmann, 1991
Vaginulina sp.
Valvulineria sp.

References

Accarie, H., Emmanuel, L., Robaszynski, F., Baudin, F., Amédro, F., Caron, M., Deconinck, J.F., 1996. La géochimie isotopique du carbone ($\delta^{13}C$) comme outil stratigraphique. Aplication à la limite Cénomanien/Turonien en Tunisie central. C. R. Acad. Sci. Paris 322, 579–586.

Accarie, H., Robaszynski, F., Amédro, F., Caron, M., Zagrarni, M.F., 2000. Stratigraphie événementielle au passage Cénomanien-Turonien dans le secteur occidental de la plate-forme de la Tunisie centrale (Formation Bahloul, région de Kalaat Senan). Ann. Mines Géol. Tunis 40, 63–80.

Alegret, L., 2007. Recovery of the deep-sea floor after the Cretaceous/Paleogene boundary event: the benthic foraminiferal record in the Basque-Cantabrian basin and in South-eastern Spain. Palaeogeogr. Palaeoclimatol. Palaeoecol. 255, 181–194.

Alegret, L., Thomas, E., Lohmann, K.C., 2012. End-Cretaceous marine mass extinction not caused by productivity collapse. Proc. Natl. Acad. Sci. 109, 728–732.

Amédro, F., Accarie, H., Robaszynski, F., 2005. Position de la limite Cénomanien-Turonien dans le Formation Bahloul de Tunisie centrale: apports intégrés des ammonites et des isotopes du carbone ($\delta^{13}C$). Eclogae Geol. Helv. 98, 151–167.

Arreguín-Rodríguez, G.J., Alegret, L., Sepúlveda, J., Newman, S., Summons, R.E., 2014. Enhanced terrestrial input supporting the *Glomospira* acme across the Paleocene-Eocene boundary in Southern Spain. Micropaleontology 60, 43–51.
Arthur, M.A., Jenkyns, H.C., Brumsack, H.J., Schlanger, S.O., 1990. Stratigraphy, geochemistry, and paleoceanography of organic carbon-rich Cretaceous sequences. In: Ginsburg, R.N., Beaudoin, B. (Eds.), Cretaceous ressources, events and rhythms: Background and plans for research. NATO ASI series, pp. 75–119.
Bernhard, J.M., 1986. Characteristic assemblages and morphologies of benthic foraminifera from anoxic, organic rich deposits: Jurassic trough Holocene. J. Foraminifer. Res. 16, 207–215.
Bjerrum, C.J., Bendtsen, J., Legarth, J.J.F., 2006. Modeling organic carbon burial during sea level rise with reference to the Cretaceous. Geochem. Geophys. Geosyst. 7, Q05008.
Bornemann, A., Norris, R.D., Friedrich, O., Beckmann, B., Schouten, R., Sinninghe-Damste, J., Vogel, J., Hofmann, P., Wagner, T., 2008. Isotopic evidence for glaciation during the Cretaceous super-greenhouse. Science 319, 951–954.
Burollet, P.F., 1956. Contribution à l'étude stratigraphique de la Tunisie Centrale. Ann. Mines Géol. Tunis 18, 1–345.
Burollet, P.F., Busson, G., 1983. Plate-forme Saharienne et Mésogée au cours du Crétacé. Notes Mem. Total-CFP 18, 17–26.
Calvert, S.E., 1990. Geochemistry and origin of the Holocene sapropel in the Black Sea. In: Ittekkot, V., Kempe, S., Michaelis, W., Spitzy, A. (Eds.), Facets of Modern Biogeochemistry. Springer, Berlin, pp. 326–352.
Calvert, S.E., Fontugne, M.R., 2001. On the late Pleistocene-Holocene sapropel record of climatic and oceanographic variability in the eastern Mediterranean. Paleoceanography 16, 78–94.
Calvert, S.E., Pedersen, T.F., 1993. Geochemistry of recent oxic and anoxic marine sediments: Implications for the geological record. Mar. Geol. 113, 67–88.
Caron, M., 1983. La spéciation chez les Foraminifères planctiques: une réponse adaptée aux contraintes de l´environnement. Zitteliana 10, 671–676.
Caron, M., Homewood, P., 1983. Evolution of early planktic foraminifers. Mar. Micropaleontol. 7, 453–462.
Caron, M., Robaszynski, F., Amédro, F., Baudin, F., Deconinck, J.F., Hochli, P., Von Salis-Perch Nielsen, K., Tribovillard, N., 1999. Estimation de la durée de l'événement anoxique global au passage Cénomanien-Turonien. Approche cyclostratigraphique dans la Formation Bahloul en Tunisie centrale. Bull. Soc. Geol. Fr. 170, 145–160.
Caron, M., Dall'Agnolo, S., Accarie, H., Barrera, E., Kauffman, E.G., Amédro, F., Robaszynski, F., 2006. High-resolution stratigraphy of the Cenomanian_Turonian boundary interval at Pueblo (USA) and wadi Bahloul (Tunisia): stable isotope and bio-events correlation. Geobios 39, 171–200.
Coccioni, R., Luciani, V., 2004. Planktonic foraminifera and environmental changes across the Bonarelli Event (OAE2, Latest Cenomanian) in its type area: a high-resolution study from the Tethyan reference Bottaccione section (Gubbio, Central Italy). J. Foraminifer. Res. 34, 109–129.
Coccioni, R., Fabbrucci, L., Galeotti, S., 1993. Terminal Cretaceous deep-water benthic foraminiferal decimation, survivorship and recovery at Caravaca (SE Spain). Paleopelagos 3, 3–24.
Corliss, B.H., 1985. Microhabitat of benthic foraminifera with deep sea sediments. Nature 314, 435–438.
Corliss, B.H., 1991. Morphology and microhabitat preferences of benthic foraminifera from the northwest Atlantic Ocean. Mar. Micropaleontol. 17, 195–236.
Corliss, B.H., Chen, C., 1988. Morphotype patterns of Norwegian deep sea benthic foraminifera and ecological implications. Geology 16, 716–719.
Eicher, D.L., Worstell, P., 1970. Cenomanian and Turonian foraminfiera from the Great Plains, United States. Micropaleontology 16, 269–324.
Erba, E., 2004. Calcareous nannofossils and Mesozoic oceanic anoxic events. Mar. Micropaleontol. 52, 85–106.
Erba, E., Bottini, C., Faucher, G., 2013. Cretaceous large igneous provinces: The effects of submarine volcanism on calcareous nannoplankton. Mineral. Mag. 77, 1044.
Erbacher, J., Huber, B.T., Norris, R.D., Markey, M., 2001. Increased thermohaline stratification as a possible cause for an ocean anoxic event in the Cretaceous period. Nature 409, 325–327.
Farrimond, P., Eglinton, G., Brassell, S.C., 1990. The Cenomanian/Turonian anoxic event in Europe: an organic geochemical study. Mar. Pet. Geol. 7, 75–89.
Fischer, A.G., Arthur, M.A., 1977. Secular variations in the pelagic realm. In: Cook, H.E. (Ed.), Deep-water carbonate environments. SEPM Sp. Pub. 25, pp. 19–50.
Flores, J.A., Sierro, F.J., Filippelli, G.M., Barcena, M.A., Pérez-Folgado, M., Vázquez, A., Utrilla, R., 2005. Surface water dynamics and phytoplankton communities during deposition of cyclic late Messinian sapropel sequences in the western Mediterranean. Mar. Micropaleontol. 56, 50–79.
Föllmi, K.B., 1995. 160 m.y. record of marine sedimentary phosphorous burial: coupling of climate and continental weathering under greenhouse and icehouse conditions. Geology 23, 859–862.
Fontanier, C., Jorissen, F.J., Licari, L., Alexandre, A., Anschutz, P., Carbonel, P., 2002. Live benthic foraminiferal faunas from the Bay of Biscay: faunal density, composition and microhabitats. Deep-Sea Res. Part 1. Oceanogr. Res. Pap. 49, 751–785.
Friedrich, O., Erbacher, J., 2006. Benthic foraminiferal assemblages from Demerara Rise (ODP Leg 207, western Tropical Atlantic): possible evidence for a progressive opening of the Equatorial Atlantic Gateway. Cretac. Res. 27, 377–397.
Friedrich, O., Erbacher, J., Wilson, P.A., Moriya, K., Mutterlose, J., 2009. Paleoenvironmental changes across the Mid Cenomanian Event in the tropical Atlantic Ocean (Demerara Rise, ODP Leg 207) inferred from benthic foraminiferal assemblages. Mar. Micropaleontol. 71, 28–40.
Gallego-Torres, D., Martínez-Ruiz, F., Paytan, A., Jiménez-Espejo, F.J., Ortega-Huertas, M., 2007. Pliocene–Holocene evolution of depositional conditions in the eastern Mediterranean: Role of anoxia vs. productivity at 632 time of sapropel deposition. Palaeogeogr. Palaeoclimatol. Palaeoecol. 246, 424–439.
Gavrilov, Y.O., Shcherbinina, E.A., Golovanova, O.V., Pokrovskii, B.G., 2013. The Late Cenomanian paleoecological event (OAE 2) in the eastern Caucasus basin of Northern Peri-Tethys. Lithol. Miner. Resour. 48, 457–488.
Gebhardt, H., Kuhnt, W., Holbourn, A., 2004. Foraminiferal response to sea level change, organic flux and oxygen deficiency in the Cenomanian of the Tarfaya Basin, southern Morocco. Mar. Micropaleontol. 53, 133–157.
Gebhardt, H., Friederich, O., Schenk, B., Fox, L., Hart, M., Wagreich, M., 2010. Paleoceanographic changes at the northern Tethyan margin during the Cenomanian-Turonian Oceanic Anoxic Event (OAE2). Mar. Micropaleontol. 77, 25–45.
Gertsch, B., Keller, G., Adatte, T., Berner, Z., Kassab, A.S., Tantawy, A.A.A., El-Sabbagh, A.M., Stueben, D., 2010. Cenomanian-Turonian transition in a shallow water sequence of the Sinai, Egypt. Int. J. Earth Sci. 99, 165–182.
Gooday, A., 2003. Benthic foraminifera (Protista) as tools in deep-water palaeoceanography: environmental influences on faunal characteristics. Adv. Biol. 46, 1–90.
Gupta, L.P., Kawahata, H., 2006. Downcore diagenetic changes in organic matter and implications for paleoproductivity estimates. Glob. Planet. Chang. 53, 122–136.
Gustafsson, M., Holbourn, A., Kuhnt, W., 2003. Changes in Northeast Atlantic temperature and carbon flux during the Cenomanian/Turonian paleoceanographic event: the Goban Spur stable isotope record. Palaeogeogr. Palaeoclimatol. Palaeoecol. 201, 51–66.
Hallam, A., 1992. Phanerozoic sea level changes. Columbia Press, New York (266 pp.).
Handoh, I.C., Lenton, T.M., 2003. Periodic mid-Cretaceous oceanic anoxic events linked by oscillations of the phosphorous and oxygen biogeochemical cycles. Glob. Biogeochem. Cycles 17. http://dx.doi.org/10.1029/2003GB002039.
Hardas, P., Mutterlose, M.J., 2007. Calcareous nannofossil assemblages of Oceanic Anoxic Event 2 in the equatorial Atlantic: Evidence of an eutrophication event. Mar. Micropaleontol. 66, 52–69.
Hardenbol, J., Thierry, J., Farley, M.B., Jacquin, T., de Graciansky, P.C., Vail, P.R., 1998. Mesozoic and Cenozoic Sequence chronostratigraphic framework of European Basins. In: Graciansky, P.C., Hardenbol, J., Jacquin, T., Vail, P.R. (Eds.), Mesozoic and Cenozoic Sequence Stratigraphy of European Basins. SEPM Sp. Publ 60, pp. 3–13.
Hart, M.B., 1996. Recovery of the food chain after the late Cenomanian extinction event. In: Hart, M.B. (Ed.), Biotic recovery from Mass Extinction Events. Geological Society of London Sp. Publ 102, pp. 265–277.
Hart, M.B., 1999. The evolution and diversity of Cretaceous planktonic foraminiferida. Geobios 32, 247–255.
Hart, M.B., Bailey, H.W., 1979. The distribution of planktonic Foraminiferida in the Mid-Cretaceous of NW Europe. In: Wiedmann, J. (Ed.), Aspekte der Kreide Europas. International Union of Geological Sciences, Series A 6, pp. 527–542.
Hemleben, C., Spindler, M., Anderson, O.R., 1989. Modern planktonic foraminifera. Springer-Verlag, Berlin (363 pp.).
Holbourn, A., Kuhnt, W., 2002. Cenomanian-Turonian palaeoceanographic change on the Kerguelen Plateau a comparison with Northern Hemisphere records. Cretac. Res. 23, 333–349.
Holbourn, A., Kuhnt, W., Erbacher, J., 2001. Benthic foraminifers from lower Albian black shales (Site 1049, ODP leg 171): evidence for a non 'uniformitarian' record. J. Foraminifer. Res. 31, 60–74.
Huber, B.T., Norris, R.D., McLeod, K.G., 2002. Deep-sea paleotemperature record of extreme warmth during the Cretaceous. Geology 30, 123–126.
Ingall, E.D., Bustin, R.M., Van Cappellen, P., 1993. Influence of water column anoxia on the burial and preservation of carbon and phosphorus in marine shales. Geochim. Cosmochim. Acta 57, 303–316.
Jarvis, I., Lignum, J.S., Groecke, D.R., Jenkyns, H.C., Pearce, M.A., 2011. Black shale deposition, atmospheric CO2 drawdown, and cooling during the Cenomanian-Turonian Oceanic Anoxic Event. Paleoceanography 26, PA3201.
Jones, R.W., Charnock, M.A., 1985. "Morphogroups" of agglutinating foraminifera. Their life position and feeding habits and potential applicability in (paleo)ecological studies. Rev. Paléobiol. 4, 311–320.
Jones, B.A., Manning, D.A.C., 1994. Comparison of geochemical indices used for the interpretation of paleoredox conditions in ancient mudstones. Chem. Geol. 111, 111–129.
Jorissen, F.J., De Stigter, H.C., Widmark, J.G.V., 1995. A conceptual model explaining benthic foraminiferal habitats. Mar. Micropaleontol. 26, 3–15.
Kaiho, K., 1994. Planktonic and benthic foraminiferal extinction events during the last 100 m.y. Palaeogeogr. Palaeoclimatol. Palaeoecol. 111, 45–71.
Kaiho, K., 1999. Evolution in the test size of deep-sea benthic foraminifera during the past 120 m.y. Mar. Micropaleontol. 37, 53–65.
Keller, G., Pardo, A., 2004. Age and environment of the Cenomanian-Turonian global stratotype section and point at Pueblo, Colorado. Mar. Micropaleontol. 51, 95–128.
Keller, G., Han, Q., Adatte, T., Burns, S.J., 2001. Paleoenvironment of the Cenomanian-Turonian transition at Eastbourne, England. Cretac. Res. 22, 391–422.
Klein, C., Mutterlose, J., 2001. Benthic foraminifera: indicators for a long-term improvement of living conditions in the late Valanginian of the NW German Basin. J. Micropalaeontol. 20, 81–95.
Kuroda, J., Ogawa, N.O., Tanimizu, M., Coffin, M.T., Tokuyama, H., Kitazato, H., Ohkouchi, N., 2007. Contemporaneous massive subaerial volcanism and late Cretaceous Oceanic Anoxic Event 2. Earth Planet. Sci. Lett. 256, 211–223.
Kuypers, M.M.M., Pancost, R.D., Nijenhuis, I.A., Sinninghe-Damste, J.S., 2002. Enhanced productivity led to increased organic carbon burial in the euxinic North Atlantic Basin during the late Cenomanian oceanic anoxic event. Paleoceanography 17, 1051.
Latimer, J.C., Filippelli, G.M., 2001. Terrigenous input and paleoproductivity in the Southern Ocean. Paleoceanography 16, 627–643.
Leckie, R., Yuretich, R.F., West, O.L.O., Finkelstein, D., Schmidt, M., 1998. Paleoceanography of the southwestern Western Interior Sea during the time of the Cenomanian-Turonian boundary (Late Cretaceous). In: Dean, W., Arthur, M.A. (Eds.), Stratigraphy

and Paleoenvironments of the Cretaceous Western Interior Seaway, USA. Society for Sedimentary Geology, Concepts in Sedimentology and Paleontology 6, pp. 101–126 (Tulsa).
Leutenegger, S., Hansen, H.J., 1979. Ultrastructural and radiotracer studies of pore function in foraminifera. Mar. Biol. 54, 11–16.
Monteiro, F.M., Pancost, R.D., Ridwell, A., Donnadieu, Y., 2012. Nutrients as the dominant control on the spread of anoxia and euxinia across the Cenomanian-Turonian oceanic anoxic event (OAE2): model-data comparison. Paleoceanography 27, PA4209.
Mort, M., Adatte, T., Föllmi, K.B., Keller, G., Steinmann, P., Matera, V., Berner, Z., Stüben, D., 2007. Phosphorous and the roles of productivity and nutrient recycling during oceanic event 2. Geology 35, 483–486.
Murray, J.W., 1991. Ecology and palaeoecology of benthic foraminifera. Longman, Harlow (397 pp.).
Nagao, S., Nakashima, S., 1992. Possible complexation of uranium with dissolved humic substances in pore water of marine-sediments. Sci. Total Environ. 118, 439–447.
Nagy, J., 1992. Environmental significance of foraminiferal morphogroups in Jurassic North Sea deltas. Palaeogeogr. Palaeoclimatol. Palaeoecol. 95, 111–134.
Nederbragt, A.J., Fiorentino, A., 1999. Stratigraphy and paleoceanography of the Cenomanian-Turonian Boundary Event in Oued Mellegue, north-western Tunisia. Cretac. Res. 20, 47–62.
Negra, M.H., Zagrarni, M.F., Hanini, A., Strasser, A., 2011. The filament event near the Cenomanian-Turonian boundary in Tunisia: filament origin and environmental signification. Bull. Soc. Géol. Fr. 182, 507–519.
Norris, R.D., Bice, K.L., Magno, E.A., Wilson, P.A., 2002. Jiggling the tropical thermostat in the Cretaceous hothouse. Geology 30, 299–302.
Peryt, D., 2004. Benthic foraminiferal response to the Cenomanian-Turonian and Cretaceous-Paleogene boundary events. Prz. Geol. 52, 827–832.
Peryt, D., Lamolda, M., 1996. Benthonic foraminiferal mass extinction and survival assemblages from the Cenomanian-Turonian Boundary Event in the Menoyo section, northern Spain. Geol. Soc. Lond. Spec. Publ. 102, 245–258.
Petrizzo, M.R., 2002. Palaeoceanographic and palaeoclimatic inferences from Late Cretaceous planktonic foraminiferal assemblages from the Exmouth Plateau (ODP Sites 762 and 763, eastern Indian Ocean). Mar. Micropaleontol. 45, 117–150.
Plewa, K., Meggers, H., Kasten, S., 2006. Barium in sediments off northwest Africa: A tracer for palaeoproductivity or meltwater events? Paleoceanography 21, PA2015.
Pogge von Strandmann, P.A.E., Jenkyns, H.C., Woodfine, R.G., 2013. Lithium isotope evidence for enhanced weathering during Oceanic Anoxic Event 2. Nat. Geosci. 6, 668–672.
Powell, W.G., Johston, P.A., Collom, C.J., 2003. Geochemical evidence for oxygenated bottom waters during deposition of fossiliferous strata of the Burgess Shale Formation. Palaeogeogr. Palaeoclimatol. Palaeoecol. 201, 249–268.
Premoli Silva, I., Sliter, W.V., 1999. Cretaceous Paleoceanography: evidence from planktonic foraminiferal evolution. In: Barrera, E., Johnson, C.C. (Eds.), Evolution of the Cretaceous ocean-climate system. Geological Society America Sp Paper 332, pp. 301–328.
Reolid, M., Martínez-Ruiz, F., 2012. Comparison of benthic foraminifera and geochemical proxies in shelf deposits from the Upper Jurassic of the Prebetic (southern Spain). J. Iber. Geol. 38, 449–465.
Reolid, M., Rodríguez-Tovar, F.J., Nagy, J., Olóriz, F., 2008. Benthic foraminiferal morphogroups of mid to outer shelf environments of the Late Jurassic (Prebetic Zone, Southern Spain): Characterisation of biofacies and environmental significance. Palaeogeogr. Palaeoclimatol. Palaeoecol. 261, 280–299.
Reolid, M., Rodríguez-Tovar, F.J., Marok, A., Sebane, A., 2012a. The Toarcian Oceanic Anoxic Event in the Western Saharan Atlas, Algeria (North African Paleomargin): Role of anoxia and productivity. Geol. Soc. Am. Bull. 124, 1646–1664.
Reolid, M., Rodríguez-Tovar, F.J., Nagy, J., 2012b. Ecological replacement of Valanginian agglutinated foraminifera during a maximum flooding event in the Boreal realm (Spitsbergen). Cretac. Res. 33, 196–204.
Robaszynski, F., Caron, M., Dupuis, C., Amédro, F., González-Donoso, J.M., Linares, D., Hardenbol, J., Gartner, S., Calandra, F., Deloffre, 1990. A tentative integrated stratigraphy in the Turonian of central Tunisia: Formations, zones and sequential stratigraphy in the Kalaat Senan area. Bull. Cent. Rech. Explor. Prod. Elf-Aquitaine 14, 213–384.
Robaszynski, F., Caron, M., Amédro, F., Dupuis, C., Hardenbol, J., González-Donoso, J.M., Linares, D., Gartner, S., 1993. Le Cénomanien de la región de Kalaat Senan (Tunisie Centrale): Litho-biostratigraphie et interprétation séquentielle. Rev. Paléobiol. 12, 351–505.
Robaszynski, F., Zargrani, M.F., Caron, M., Amédro, F., 2010. The global bio-events at the Cenomanian-Turonian transition in the reduced Bahloul Formation of Bou Ghanem (central Tunisia). Cretac. Res. 31, 1–15.
Robertson, A.K., Filippelli, G.M., 2008. Paleoproductivity variations in the eastern equatorial Pacific over glacial timescales: American Geophysical Union Fall Meeting 2008, Abstract PP33C-1576.
Saïdi, F., Ben Ismaïl, M.H., M'Rabat, A., 1997. Le Turonien de Tunisie centro-occidentale: facies, paléogéographie séquentielle d'une plate-form. Cretac. Res. 18, 63–85.
Sarmiento, J.L., Herbert, T.D., Toggweiler, J.R., 1988. Causes of anoxia in the world ocean. Glob. Biogeochem. Cycles 2, 115–128.
Schlanger, S.O., Jenkyns, H.C., 1976. Cretaceous oceanic anoxic events, causes and consequences. Geol. Mijnb. 55, 179–184.
Schlanger, S.O., Arthur, M.A., Jenkyns, H.C., Scholle, P.A., 1987. The Cenomanian-Turonian oceanic anoxic event, I. Stratigraphy and distribution of organic-rich beds and the marine $\delta^{13}C$ excursión. In: Brooks, J., Fleet, A.J. (Eds.), Marine Petroleum Source Rocks. Special Publication, Geol. Soc. London 26, pp. 371–399.
Scholle, P.A., Arthur, M.A., 1980. Carbon isotope fluctuations in Cretaceous pelagic limestones: potential stratigraphic and petroleum exploration tool. AAPG Bull. 64, 67–87.
Scopelliti, G., Bellanca, A., Coccioni, R., Luciani, V., Neri, R., Baudin, F., Chiari, M., Marcucci, M., 2004. High-resolution geochemical and biotic records of the Tethyan 'Bonarelli Level' (OAE2, latest Cenomanian) from the Calabianca-Guidaloca composite section, northwestern Sicily, Italy. Palaeogeogr. Palaeoclimatol. Palaeoecol. 208, 293–317.
Scott, R.W., 2003. High resolution North African Cretaceous stratigraphy: status. In: Gili, E., Negra, M.H., Skelton, W. (Eds.), Cretaceous carbonate platform systems. Nato Science Series 28, pp. 1–17.
Sen, A.K., Filippelli, G.M., Flores, J.A., 2008. An application of wavelet analysis to palaeoproductivity records from the Southern Ocean. Comput. Geosci. 35, 1445–1450.
Sliter, W.V., 1975. Foraminiferal life and residue assemblages from Cretaceous slope deposits. Geol. Soc. Am. Bull. 86, 897–906.
Soua, M., Zaghbib-Turki, D., Ben Jemia, H., Smaoui, J., Boukadi, A., 2011. Geochemical record of the Cenomanian-Turonian anoxic event in Tunisia: Is it correlative and isochronous to the biotic signal? Acta Geol. Sin. 85, 801–840.
Sprong, J., Kouwenhoven, T.J., Bornemann, A., Dupuis, C., Speijer, R.P., Stassen, P., Steurbaut, E., 2013. In search of the Latest Danian Event in a paleobathymetric transect off Kasserine Island, north-central Tunisia. Palaeogeogr. Palaeoclimatol. Palaeoecol. 379, 1–16.
Su, W., Wang, Y., Cramer, B.D., Munnecke, A., Li, Z., Fu, L., 2008. Preliminary estimation of palaeoproductivity via TOC and habitat types: which method is more reliable? A case study on the Ordovician/Silurian transitional black shales of the Upper Yangtze Platform, South China. J. China Univ. Geosci. 19, 534–548.
Sun, Y.B., Wu, F., Clemens, S.C., Oppo, D.W., 2008. Processes controlling the geochemical composition of the South China Sea sediments during the last climatic cycle. Chem. Geol. 257, 234–249.
Thierry, J., 2000. Middle Callovian (157–155 Ma). In: Dercourt, J., Gaetani, M., Vrielynck, B., Barrier, E., Biju-Duval, B., Brunet, M.-F., Cadet, J.P., Crasquin, S., Sandulescu, M. (Eds.), Atlas Peri-Tethys palaeogeographical maps. CCGM/CGMW, Paris, pp. 71–97.
Tribovillard, N., Algeo, T., Lyons, T., Riboulleau, A., 2006. Trace metals as palaeoredox and palaeoproductivity proxies: an update. Chem. Geol. 232, 12–32.
Trivobillard, N., Algeo, T.J., Baudin, F., Riboulleau, A., 2012. Analysis of marine environmental conditions based on molybdenum-uranium covariation – Applications to Mesozoic paleoceanography. Chem. Geol. 324–325, 46–58.
Tsandev, I., Slomp, C.P., 2009. Modeling phosphorous cycling and carbon burial during Cretaceous Oceanic Anoxic Events. Earth Planet. Sci. Lett. 286, 71–79.
Turgeon, S.C., Brumsack, H.J., 2006. Anoxic vs dysoxic events reflected in sediment geochemistry during the Cenomanian-Turonian Boundary Event (Cretaceous) in the Umbria-Marche basin of central Italy. Chem. Geol. 234, 321–339.
Turgeon, S.C., Creaser, R.A., 2008. Cretaceous oceanic anoxic event 2 triggered by a massive magmatic episode. Nature 454, 323–326.
Tyszka, J., 1994. Response of Middle Jurassic benthic foraminiferal morphogroups to dysoxic/anoxic conditions in the Pieniny Klippen Basin, Polish Carpathians. Palaeogeogr. Palaeoclimatol. Palaeoecol. 110, 55–81.
Valentine, J.W., 1973. Evolutionary ecology of the marine biosphere. Prentice Hall, Englewood NJ (511 pp.).
Van Cappellen, P., Ingall, E.D., 1994. Benthic phosphorus regeneration, net primary production, and ocean anoxia—A model of the coupled marine biogeochemical cycles of carbon and phosphorus. Paleoceanography 9, 677–692.
Van der Zwaan, G.J., Duijnstee, I.A.P., Den Dulk, M., Ernst, S.R., Jannink, N.T., Kouwenhoven, T.J., 1999. Benthic foraminifers: proxies or problem? A review of paleoecological concepts. Earth Sci. Rev. 46, 213–236.
Wagner, T., Wallmann, K., Herrle, J.O., Hofmann, P., Stuesser, L., 2007. Consequences of moderate 25,000 yr lasting emission of light CO_2 into the mid-Cretaceous ocean. Earth Planet. Sci. Lett. 259, 200–211.
Wang, C.S., Hu, X.M., Jansa, L., Wan, X.Q., Tao, R., 2001. The Cenomanian-Turonian anoxic event in southern Tibet. Cretac. Res. 22, 481–490.
Widmark, J.G.V., Speijer, R.P., 1997. Benthic foraminiferal faunas and trophic regimes at the terminal Cretaceous Tethyan seafloor. Palaios 12, 354–371.
Wignall, P.B., Myers, K.J., 1988. Interpreting the benthic oxygen levels in mudrocks: a new approach. Geology 16, 452–455.
Zaghbib-Turki, D., Soua, M., 2013. High resolution biostratigraphy of the Cenomanian-Turonian interval (OAE2) based on planktonic foraminiferal bioevents in North-Central Tunisia. J. Afr. Earth Sci. 78, 97–108.
Zagrarni, M.F., Negra, M.H., Hanini, A., 2008. Cenomanian-Turonian facies and sequence stratigraphy, Bahloul Formation, Tunisia. Sediment. Geol. 204, 18–35.
Zheng, X.Y., Jenkyns, H.C., Gale, A.S., Ward, D.J., Henderson, G.M., 2013. Changing ocean circulation and hydrothermal inputs during Ocean Anoxic Event 2 (Cenomanian-Turonian): Evidence from Nd-isotopes in the European shelf sea. Earth Planet. Sci. Lett. 375, 338–348.
Zhou, L., Wignall, P.B., Su, J., Feng, Q., Xie, S., Zhao, L., Huang, J., 2012. U/Mo ratios and $\delta^{98/95}Mo$ as local and global redox proxies during mass extinction events. Chem. Geol. 324–325, 99–197.